Identifying the Minimum Number of Subadult Individuals in Grave 6 of the Wadi Faynan 100 Cemetery, Jordan

by

Amanda Kubiak

A thesis

presented to the University of Waterloo

in fulfillment of the

thesis requirement for the degree of

Master of Arts

in

Public Issues Anthropology

Waterloo, Ontario, Canada, 2025

© Amanda Kubiak 2025

Authors Declaration

I hereby declare that I am the sole author of this thesis. This is a true copy of the thesis, including any required final revisions, as accepted by my examiners.

I understand that my thesis may be made electronically available to the public.

Abstract

Estimating the Minimum Number of Individuals (MNI) in commingled and fragmentary assemblages is particularly difficult for subadults, whose remains are often fragile and incomplete. This thesis applies a modified Landmark System to the subadult assemblage from Grave 6 at Wadi Faynan 100, an Early Bronze Age IB site in southern Jordan, to subadult MNI estimation. The analysis identified a minimum of 22 subadults, ranging from perinatal to late adolescence. These findings demonstrate the value of the Landmark System for subadult remains, expanding the methodological toolkit available for osteologists working with highly fragmentary collections. Beyond methodology, this study contributes to understanding Early Bronze Age mortuary practice in the southern Levant.

Acknowledgements

First and foremost, I would like to thank my advisor, Dr. Alexis Dolphin, whose guidance, patience, and encouragement carried me through every stage of this project. You have helped me become a better writer, researcher, and student. I am also deeply grateful to my committee, whose feedback and support helped me achieve my goals.

To my lab mates and peers, thank you for sharing a positive workspace and for making the work lighter with your company and support. I have learned an endless amount from all of you.

To my friends and family, thank you for keeping my spirits high when I needed it most, always checking in, and making sure I took care of myself. I am forever grateful to have you in my life.

I would also like to thank the University of Waterloo for the opportunity to pursue a graduate degree in anthropology, and to those who helped excavate the subadult remains in 2023.

Finally, and most importantly, I would like to thank the individuals whose remains I studied. It has been a privilege to learn from you, thank you for helping me. May you rest easy once more.

Contents

Authors Declaration ii

Abstract iii

Acknowledgements iv

List of Figures vii

List of Tables x

Chapter 1: Introduction 1

1.1 ***Research Design and Scope*** 1

1.2 ***Ethics*** 2

1.3 ***Public Issues*** 5

Chapter 2: Wadi Faynan 100 9

2.1 ***The Early Bronze Age in Jordan*** 9

2.1.1 ***Wadi Faynan 100*** 11

2.1.2 ***Burials at Wadi Faynan 100*** 12

2.2 ***Previous Research with Human Remains from WF100*** 15

Chapter 3: Minimum Number of Individuals (MNI) Methods 16

3.1 ***Traditional MNI (White 1953)*** 16

3.2 ***Zonation Method*** 18

3.3 ***Landmark System*** 20

3.4 ***Age-at-Death (AAD) Methods*** 23

3.5 ***Landmark Modification for Subadults*** 25

Chapter 4: Materials 28

4.1 ***The Assemblage*** 28

4.1.1 ***Long bones*** 28

4.1.2 ***Cranial Bones*** 29

4.1.3 ***Irregular Bones, Flat Bones*****, and** ***Vertebral Elements*** 29

4.1.4 ***Hand, Wrist, Foot, and Ankle Bones*** 30

4.2 ***Estimation of Age-at-Death*** 31

Chapter 5: Results 33

5.1 ***Minimum Number of Individuals (MNI)*** 33

5.2 ***Age-at-Death Estimates (AAD)*** 38

Chapter 6 – Discussion 80

6.1 ***Minimum Number of Individuals (MNI)*** 80

6.1.1 ***Limitations for estimating MNI*** 81
6.2 ***Age-At-Death (AAD)*** 82
6.2.1 ***Limitations for Estimating Age-At-Death*** 83
Chapter 7: Conclusion 85
References 87
Appendix A – ***Landmark System Reference Guide*** 93
Appendix B – ***Photos of the Wadi Faynan 100 Grave 6 Subadult Collection*** 115

List of Figures

Figure 1. Wadi Faynan 100 site plan (Adams et al. 2023, pg. 1) 12
Figure 2. Grave 6 opening facing north (Adams et al. 2023, pg. 5) 14
Figure 3. Grave 6 closing facing south (Adams et al. 2023, pg. 5) 14
Figure 4. Right Humerus, posterior and anterior views with codified zones (Knüsel and Outram, 2004, pg 90). 19
Figure 5. Right scapula, anterior, lateral, and posterior views, with codified landmarks (Mack et al., 2015, pg 4). 21
Figure 6. Endochondral bone growth model. (Wikimedia Commons, 2025). 24
Figure 7. Intramembranous bone development model. (Carstens, 2023, pg 339). 25
Figure 8. Skeletal elements from Grave 6, Locus 1 (estimated age range: 5–13 years), highlighted in blue. Elements may represent one or more subadults. 41
Figure 9. Skeletal elements from Grave 6, Locus 2 (estimated age range: 1-5 years), highlighted in blue. Elements may represent one or more subadults. 44
Figure 10. Skeletal elements from Grave 6, Locus 3 (estimated age range: 6-12 years), highlighted in blue. Elements may represent one or more subadults. 46
Figure 11. Skeletal elements from Grave 6, Locus 3 (estimated age range: 12-18 years), highlighted in blue. Elements may represent one or more subadults. 47
Figure 12. Skeletal elements from Grave 6, Locus 3 (estimated age range: ~5 years), highlighted in blue. Elements may represent one or more subadults. 49
Figure 13. Skeletal elements from Grave 6, Locus 3 (estimated age range: 0-2 years), highlighted in blue. Elements may represent one or more subadults. 50
Figure 14. Skeletal elements from Grave 6, Locus 5 (estimated age range: 10-22 years), highlighted in blue. Elements may represent one or more subadults. 52
Figure 15. Skeletal elements from Grave 6, Locus 5 (estimated age range: 10-22 years), highlighted in blue. Elements may represent one or more subadults. 56
Figure 16. Skeletal elements from Grave 6, Locus 5 (estimated age range: 10-22 years), highlighted in blue. Elements may represent one or more subadults. 59
Figure 17. Skeletal elements from Grave 6, Locus 5 (estimated age range: 3-9 years), highlighted in blue. Elements may represent one or more subadults. 61
Figure 18. Skeletal elements from Grave 6, Locus 5 (estimated age range: 9-20 years), highlighted in blue. Elements may represent one or more subadults. 63
Figure 19. Skeletal elements from Grave 6, Locus 5 (estimated age range: 40 weeks - 3 years), highlighted in blue. Elements may represent one or more subadults. 64
Figure 20. Skeletal elements from Grave 6, Locus 5 (estimated age range: 2-8 years), highlighted in blue. Elements may represent one or more subadults. 66
Figure 21. Skeletal elements from Grave 6, Locus 5 (estimated age range: 2-6 years), highlighted in blue. Elements may represent one or more subadults. 68
Figure 22. Skeletal elements from Grave 6, Locus 5 (estimated age range: 2-5 years), highlighted in blue. Elements may represent one or more subadults. 69
Figure 23. Skeletal elements from Grave 6, Locus 5 (estimated age range: 12-18 years), highlighted in blue. Elements may represent one or more subadults. 70

Figure 24. Skeletal elements from Grave 6, Locus 5 (estimated age range: ~8 years), highlighted in blue. Elements may represent one or more subadults. 71
Figure 25. Skeletal elements from Grave 6, Locus 5 (estimated age range: 5-14 years), highlighted in blue. Elements may represent one or more subadults. 72
Figure 26. Skeletal elements from Grave 6, Locus 5 (estimated age range: ~8 years), highlighted in blue. Elements may represent one or more subadults. 73
Figure 27. Skeletal elements from Grave 6, Locus 5 (estimated age range: 5-12 years), highlighted in blue. Elements may represent one or more subadults. 74
Figure 28. Skeletal elements from Grave 6, Locus 5 (estimated age range: 0-3 years), highlighted in blue. Elements may represent one or more subadults. 76
Figure 29. Skeletal elements from Grave 6, Locus 5 (estimated age range: 1.5-3 years), highlighted in blue. Elements may represent one or more subadults. 77
Figure 30. Skeletal elements from Grave 6, Locus 5 (estimated age range: ~5 years), highlighted in blue. Elements may represent one or more subadults. 78
Figure 31. Pars Basilaris (A) and Pars Lateralis (B) Elements are shown before fusing with the occipital bone. Internal View. 93
Figure 32. Left Temporal (A). Internal View. 93
Figure 33. Vertebrae, General Neural Arch (A). Inferior View. Image based on Cervical Vertebra neural arch. 94
Figure 34. Vertebrae, General Centrum (Body) (A) Superior View. Image based on Lumbar Vertebra centrum. 94
Figure 35. Left Os coxa. A (ilium), B (pubis), C (ischium), a (iliac crest), b (pubic symphysis), c (lunate surface). Lateral View. 95
Figure 36. Left Scapula. A (scapular spine), B (acromion process), C (medial boarder), D (lateral boarder), E (glenoid cavity). Left = Anterior, Right = Posterior View. 96
Figure 37. Sternum. A (Manubrium). Anterior View. 97
Figure 38. Left Clavicle. A (Medial epiphysis), B (shaft). Top = Superior View, Bottom = Metaphyseal View (left) and Medial View (right). 98
Figure 39. Left Humerus. A (Proximal epiphysis/head), B (shaft), c (capitulum), d (trochlea). Anterior View. 99
Figure 40. Left Ulna. A (proximal epiphysis), B (Shaft), C (distal epiphysis). Anterior View... 100
Figure 41. Left Radius. A (proximal epiphysis), B (Shaft), C (distal epiphysis). Anterior View. 101
Figure 42. Right Metacarpal, General. A (Metacarpal), B (Metacarpal epiphysis). Dorsal View of Shaft. Top Epiphysis = Distal View, Bottom Epiphysis= Proximal Views. 102
Figure 43. Left Hand of subadult. A (phalanx) B (Phalanx epiphysis). Shafts = Dorsal View; Epiphyses = Proximal View. 103
Figure 44. Left Scaphoid. 103
Figure 45. Left Lunate. 104
Figure 46. Left Pisiform. 104
Figure 47. Left Triquetral. 104
Figure 48. Left Hamate. 105
Figure 49. Left Trapezium. 105

Figure 50. Left Trapezoid. 106
Figure 51. Left Capitate. 106
Figure 52. Left Femur. A (Head/proximal epiphysis), B (greater trochanter), C (lesser trochanter), D (neck), E (Shaft), F (Distal epiphysis), G (medial condyle, H (lateral condyle), I (intercondylar fossa). Anterior View..... 107
Figure 53. Left Tibia. A (proximal epiphysis), B (shaft), C (distal epiphysis). Anterior View... 108
Figure 54. Left Fibula. A (proximal epiphysis), B (shaft), C (distal epiphysis). Anterior View. 109
Figure 55. Left Patella. Left = Anterior View, Right = Posterior View. 110
Figure 56. Left Talus. Inferior View.....110
Figure 57. Left Calcaneus. A (calcaneus epiphysis). Superior View. 111
Figure 58. Left Cuboid. Dorsal View.....111
Figure 59. Left Navicular. Left = Proximal View, Right = Distal View. 112
Figure 60. Left First Cuneiform. Lateral View. 112
Figure 61. Left Second Cuneiform. Lateral View.....112
Figure 62. Left Third Cuneiform. Medial View.....113
Figure 63. Left Subadult foot. A (Phalanx), B (Phalanx epiphysis). Shafts = Dorsal View, Epiphyses = Proximal View. 113
Figure 64. Right Metatarsal general. A (Metatarsal), B (Metatarsal epiphysis). Shaft = Dorsal View, Epiphysis Top = Distal View, Epiphysis Bottom = Proximal View.....114
Figure 65. Lateral Border of Subadult Scapula 115
Figure 66. Subadult Pars Lateralis 116
Figure 67. Subadult Miscellaneous Squama 116
Figure 68. Subadult Miscellaneous Long Bone Fragment.....117

List of Tables

Table 1. Grave 6, Locus 1 MNI Results. Sides are indicated as L (left), R (right), or N/A for unsided. 33
Table 2. Grave 6, Locus 2 MNI Results, Sides are indicated as L (left), R (right), or N/A for unsided.\ 34
Table 3. Grave 6, Locus 3 MNI Results, Sides are indicated as L (left), R (right), or N/A for unsided. 34
Table 4. Grave 6, Locus 5 MNI Results, Sides are indicated as L (left), R (right), or N/A for unsided. 37
Table 5. Grave 6, Locus 6 MNI Results, Sides are indicated as L (left), R (right), or N/A for unsided. 38
Table 6. Skeletal elements from Grave 6, Locus 1 (estimated age range: 5-12). Sides are indicated as L (left), R (right), or N/A for unsided. 41
Table 7. Skeletal elements from Grave 6, Locus 1 (estimated age range: 10-13). Sides are indicated as L (left), R (right), or N/A for unsided. 42
Table 8. Skeletal elements from Grave 6, Locus 2 (estimated age range: 1-5 years). Sides are indicated as L (left), R (right), or N/A for unsided. 44
Table 9. Skeletal elements from Grave 6, Locus 3 (estimated age range: 6-12 years). Sides are indicated as L (left), R (right), or N/A for unsided. 46
Table 10. Skeletal elements from Grave 6, Locus 3 (estimated age range: 12-18 years). Sides are indicated as L (left), R (right), or N/A for unsided. 48
Table 11. Skeletal elements from Grave 6, Locus 3 (estimated age range: 3-5 years). Sides are indicated as L (left), R (right), or N/A for unsided. 49
Table 12. Skeletal elements from Grave 6, Locus 3 (estimated age range: 0-2 years). Sides are indicated as L (left), R (right), or N/A for unsided. 50
Table 13. Skeletal elements from Grave 6, Locus 5 (estimated age range: 10-20 years). Sides are indicated as L (left), R (right), or N/A for unsided. 56
Table 14. Skeletal elements from Grave 6, Locus 5 (estimated age range: 10-20 years). Sides are indicated as L (left), R (right), or N/A for unsided. 58
Table 15. Skeletal elements from Grave 6, Locus 5 (estimated age range: 10-20 years). Sides are indicated as L (left), R (right), or N/A for unsided. 60
Table 16. Skeletal elements from Grave 6, Locus 5 (estimated age range: 3-9 years). Sides are indicated as L (left), R (right), or N/A for unsided. 62
Table 17. Skeletal elements from Grave 6, Locus 5 (estimated age range: 9-20 years). Sides are indicated as L (left), R (right), or N/A for unsided. 64
Table 18. Skeletal elements from Grave 6, Locus 5 (estimated age range: 40 weeks - 3 years). Sides are indicated as L (left), R (right), or N/A for unsided. 65
Table 19. Skeletal elements from Grave 6, Locus 5 (estimated age range: 2-8 years). Sides are indicated as L (left), R (right), or N/A for unsided. 67
Table 20. Skeletal elements from Grave 6, Locus 5 (estimated age range: 2-6 years). Sides are indicated as L (left), R (right), or N/A for unsided. 68

Table 21. Skeletal elements from Grave 6, Locus 5 (estimated age range: 2-5 years). Sides are indicated as L (left), R (right), or N/A for unsided. 69
Table 22. Skeletal elements from Grave 6, Locus 5 (estimated age range: 12-18 years). Sides are indicated as L (left), R (right), or N/A for unsided. 70
Table 23. Skeletal elements from Grave 6, Locus 5 (estimated age range: ~8 years). Sides are indicated as L (left), R (right), or N/A for unsided. 71
Table 24. Skeletal elements from Grave 6, Locus 5 (estimated age range: 5-14 years). Sides are indicated as L (left), R (right), or N/A for unsided. 72
Table 25. Skeletal elements from Grave 6, Locus 5 (estimated age range: ~8 years). Sides are indicated as L (left), R (right), or N/A for unsided. 73
Table 26. Skeletal elements from Grave 6, Locus 5 (estimated age range: 5-12 years). Sides are indicated as L (left), R (right), or N/A for unsided. 75
Table 27. Skeletal elements from Grave 6, Locus 5 (estimated age range: 0-3 years). Sides are indicated as L (left), R (right), or N/A for unsided. 77
Table 28. Skeletal elements from Grave 6, Locus 5 (estimated age range: 1.5-3 years). Sides are indicated as L (left), R (right), or N/A for unsided. 78
Table 29. Skeletal elements from Grave 6, Locus 5 (estimated age range: ~5 years). Sides are indicated as L (left), R (right), or N/A for unsided. 79

Chapter 1: Introduction

1.1 *Research Design and Scope*

Establishing the Minimum Number of Individuals (MNI) estimation in osteological assemblages is essential for demographic reconstruction, yet persistent challenges are faced when dealing with fragmentary and commingled remains, particularly with subadults. This study demonstrates that the Landmark System is an effective method for refining minimum number of individuals (MNI) estimates in fragmentary and commingled subadult assemblages, as shown through its application to Grave 6 at Wadi Faynan 100, Jordan. The traditional MNI method published by Theodore E. White (1953), and the newer Zonation MNI Method published by Christopher J. Knüsel and Alan Outram (2004), have been criticized for double counting individuals, reliance on complete bones, and biased estimates with smaller samples (Lambacher et al. 2016). These limitations are pronounced when working with subadult remains, as they are inherently more sensitive to taphonomic forces and breakage (Morton and Lord 2001), as well as being easily mistaken for detritus or faunal remains (Lewis 2007). The Landmark System (Mack et al. 2015), offers a promising alternative for analyzing commingled and fragmentary collections, as it does not depend on complete skeletal elements (Lambacher et al. 2016; Dominguez-Rodrigo 2011). However, the application to subadult MNI estimation remains largely unexplored, representing a significant gap in the methodology. This study presents the application of the Landmark System with a focus on subadult remains for the MNI estimation in a commingled subadult assemblage from Grave 6 at the Wadi Faynan 100 cemetery in Jordan.

Wadi Faynan 100 is an Early Bronze Age IB (3300 BCE-3000 BCE) site of interest due to its connection to early copper metallurgic practices and the impacts they can have on an individual's health (Adams et al. 2023). By applying the Landmark System to estimate the subadult MNI, this

research will help contribute to a more comprehensive understanding of the possible subadult demographic structure of Wadi Faynan 100. This crucial piece of information will contribute foundational data that can be used by researchers to help assess the potential impacts copper metallurgy had on the population health and mortality. Therefore, this study offers valuable contributions to both osteological subadult methodology and the understanding of life and death at Wadi Faynan 100.

1.2 *Ethics*

Within this study, it is important to recognize ethical concerns regarding the study of human remains. Prominent criticisms are focused towards the individual and their cultural beliefs versus their value for research and learning by present and future generations (Licata et al. 2020; Kreissl Lonfat et al. 2015). It is a battle between the value of knowledge for the greater population versus the value of cultural beliefs for individuals and their communities. A large issue stems from the display of bodies in museums and the collection of bodies in academic assemblages for research, with scholars learning anatomy or how disease impacts bone structure. On one side, the display of individuals for the public can be seen as insensitive or disrespectful towards the body's autonomy and an individual's dignity post-mortem. It raises questions of the ownership of a body, respect of burial practices and beliefs, and proper treatment, storage, and conservation of skeletal remains (Licata et al. 2020). Furthermore, these concerns are heightened when processing and viewing subadult individuals. Subadults are under the care of their parents or suitable adult guardian for protection, and their inclusion in activities needs adult permission. When displaying the remains of a subadult individual, ethical questions arise as to whether permission should be sought from descendant communities, cultural stakeholders, or institutional ethics boards (Squires et al. 2020).

On the other side, using bodies for research helps the living to learn about the past, our own body, and its nature in decomposition, disease, and death. The study of human remains has helped answer questions of our evolution, dietary needs, impacts disease can have on the skeletal system, and bone development and growth (Licata et al. 2020). Additionally, there are ethical guidelines in place by multiple organizations to help combat the unethical treatment of remains (The Tri-council Research Agency (2022), the Canadian Anthropology Association (CAA 2022), the Canadian Association for Biological Anthropology (CABA-ACAB 2019), the Canadian Museums Association (CMA 1999), the American Anthropological Association (AAA 2012), the Society for American Archaeology (SAA 2021), and the British Association for Biological Anthropology and Osteoarchaeology (BABAO 2017).

This study was undertaken at a Canadian research institution (University of Waterloo); therefore, the presence of human remains requires the observation of Canadian guidelines. These guidelines have been established by organizations such as the Canadian Museum Association (CMA), the Tri-council research agency, the Canadian Anthropology Association (CAA), and the Canadian Association for Biological Anthropology (CABA-ACAB). These organizations emphasize that the handling, display, storage, and/or treatment of human remains or culturally sensitive objects must adhere to the originating community's standards (Canadian Museums Association 1999; Parks Canada Agency 2022; CAA 2022; CABA-ACAB 2019; Canadian Institutes of Health Research 2022; Natural Sciences and Engineering Research Council of Canada 2022; and the Social Sciences and Humanities Research Council of Canada 2022). Following the originating communities' standards will cause differences in how remains are treated; therefore, a base standard has been set for treatment of remains and the individual researching, with additional regulations added based on what community is being represented. In

Canada human remains must be treated with the utmost respect by the researcher as the remains are fragile, non-renewable, and finite. In this specific context, I interpret the utmost respect means ensuring I approached the handling and care of these remains with a commitment to upholding the physical integrity and their value as past individuals.

This study examines human remains from Wadi Fayan 100, an archaeological site in Jordan, therefore additional standards and guidelines were consulted. The Department of Antiquity (DoA) in Jordan treats archaeological human remains much differently than what is commonly observed today in Western countries. Under the Law of Antiquities (2004), human remains are listed as an antiquity if the date of origin is before AD 600, along with material culture such as sculptures, coins, and pottery (Department of Antiquities of Jordan 2004, Acor Jordan 2023; Sheridan 2017). Human remains are not categorized differently than artifacts, but rather as artifacts themselves. The DoA of Jordan requires a list, short description, and picture of any antiquity that is in a researcher's care (Department of Antiquities of Jordan 2004).

With respect to Canadian and Jordanian guidelines for human remains, the qualitative identification and assessment of the subadult WF100 remains was carried out with care towards the individual to avoid prevent further damage and preserve crucial contextual data. With respect to the preservation of this assemblage, any inconclusive or limited results found within this study may be attributed to the delicate nature of these approximately 5,000-year-old remains, and any previous damage inflicted upon them through burial practices, looting, or excavation methods. Although descendant community consultation is not applicable to WF100, The Barqa Landscape Project (BLP) members have worked with many members of the Faynan community for over 30 years. Researchers and community members regularly work together at excavation sites, co-sponsor community events, communicate via telephone, internet and social media, and BLP

members provide public presentations of results within the village of Faynan near WF100 (Alexis Dolphin, personal communication, June 30, 2025).

1.3 *Public Issues*

This thesis serves to address the public issues through ethical, cultural, and community considerations of those living in proximity to WF100 today, while also addressing a gap in research methodologies for commingled and fragmentary remains.

Often in Near Eastern archaeology, human remains are not discussed prominently. The majority of burials are from a commingled context, which can prove more difficult to work with, especially given the focus on 'osteobiography' and individuation in bioarchaeology (Sheridan 2017; Ullinger et al. 2013; Ortner and Frolich 2007). Commingled remains typically require multiple methodologies to gather important and useful information, taking time and resources that might not be available for specific projects. When human remains are discussed, commingled remains are glanced over to prioritize singular burials that can gather information on one individual, or large burials that provide enough skeletal material to gather information on diet and disease. Specific examples include those excavated from Jebel al-Mutawwaq and Bab edh-Dhra, which have been subject to intensive work and have provided a wealth of information about the Early Bronze Age in the area now known as Jordan (Sheridan et al. 2014).

Jebel al-Mutawwaq highlights some of the hesitancy surrounding the study of human remains at Jordanian archaeological sites. Most of the literature focuses on the megalithic structures, the Dolmen field, and pottery finds within the domestic structures (Fernández-Tresguerres Velasco 2001; Fernández-Tresguerres Velasco 2008; Muniz et al. 2016), while briefly commenting on the human remains - discussing their condition, where they were found (e.g. Dolmen 317 and Cave

1012), what bones remained, and possible reasons for the fragmentation and absence of more remains.

Dolmen 317 received some recognition; it is a tomb which contained a skull, an assortment of postcranial bones, and two funerary objects. An estimated five individuals were buried in this tomb, including three adults, one subadult, and one juvenile (Polcaro et al. 2014). Nevertheless, the study prioritizes the pottery, tools, and the burial structure over osteological analysis. As noted in the article "the fragmented state of preservation of a large part of the sample resulted in a partial, albeit interesting, analysis of human remains" (Polcaro et al. 2014, 12).

Similarly, in Cave 1012, approximately 10 individuals were found, however, the remains were crushed from a roof collapse. The cave was divided into 6 phases of use, of which phases 4 through 6 are interpreted as funerary. Yet, the human remains discovered received little attention in this article as well, with only small mentions of disarticulated piles of skulls and long bones during phase occupations (Polcaro and Muniz 2022).

Unlike Jebal al-Mutawwaq, Bab edh-Dhra is unique with burials dated to all periods of the Early Bronze Age, and provides the largest collection of skeletal remains from the EBA IA period. Examination of the human remains from this site has produced insight on mobility (Sheridan et al. 2014), diet (Ullinger et al. 2013), and disease (Ortner and Frolich 2007) during the Early Bronze Age. Sheridan and colleagues (2014) studied non-metric indicators of roughly 512 individuals from the EBA IA and 2363 individuals from the EBA II-III. The goal was to determine the mobility of the population, and identify changes in their mobility throughout different periods in the EBA. It was discovered the EBA IA sample was more diverse in age distribution and genetic relatedness than the EBA II-III sample, with the EBA II-III sample suggesting a multigenerational tomb with large extended family was found. Ullinger and

colleagues (2013) focused on the diet of the EBA populations from Bab edh-Dhra, examining dental caries from individuals 12 years or older. No individuals were able to be determined from the degree of commingling present. Sixty-six samples from the EBA IA were collected and 219 EBA II and III samples were collected. From the samples collected, it was determined a moderate level of dental disease was present during the EBA at Bab edh-Dhra, and their diet relied on cultivated crops with some wild plants still being eaten. There was no significant change recorded from the EBA IA sample to the EBA II-III sample. A third avenue of research was pursued by Ortner and Frolich (2007), collecting data on disease in the EBA IA population around Bab edh-Dhra. Three hundred and seventy-three shaft tombs were excavated with neonates to elders populating the sample. Of these 373 burials, 48% of the sample had died before reaching 15 years old. The life expectancy at birth was calculated to be 21.36 years old (Ortner and Frolich 2007), and most common pathology found was trauma, followed by infection, osteoarthritis, metabolic diseases, benign tumors, and congenital diseases.

Upon review of the bioarchaeological analyses of Early Bronze Age I sites in Jordan, there are several observations that may be made regarding the state of bioarchaeology in the Southern Levant. While some sites like Bab edh-Dhra are rich in bioarchaeological analysis, others are difficult to find. This is not surprising due to works like Sheridan (2017, 2019) discussing the limitations present in the analysis of human remains. Furthermore, Sheridan states the multitude of challenges that researchers are faced when working with commingled collections from the Near East. First, finding literature on remains is challenging as most publications choose to focus on other issues, and mention human remains only briefly in appendices, or ignore them completely (Sheridan 2017; Sheridan 2019). This complicates the search for human remains, and can lack sufficient necessary detail. A second challenge faced is the treatment of remains from

previous excavations. They often lay within their original excavation bags lacking further analysis, isolating human remains from study (Sheridan 2017).

Beyond the methodological and publication challenges, research at sites such as WF100 can highlight the unique history of archaeological sites, and can stimulate tourism and economic support for Jordans archaeological heritage (Radziwiłko et al. 2020; van den Dries 2021; Tirpan 2022). Research also creates jobs for the local communities, helping both the researchers navigate the area and local members of the community get involved with those visiting their home. Local members can also gain financial compensation for owning private property with archaeological interest. Financial incentives for these private land owners are associated with the local and federal government programs for cultural heritage protection programs (Kafafi 2021; Ronza 2023).

This research addresses the gap in research methodologies as the traditional methodology (White 1953) used to estimate MNI requires mostly complete skeletal elements. This excludes deteriorated or commingled collections from demographic research, as noted by Sheridan (2017). The Landmark MNI estimation method addresses this gap and grants researchers the ability to revisit previous collections. This expands of the ability of researchers to study poorly preserved and comingled collections, potentially leading to new insights of past populations. This research will serve those in the academic sphere, such as osteologists, archaeologists, forensic anthropologists, and museum curators as it addresses limitations of common research avenues and basic population demographic data. Furthermore, this method will indirectly serve the broader public as it increases the knowledge researchers can gain from past populations, informing them of our current understanding of human history and current efforts to improve our research.

Chapter 2: Wadi Faynan 100

2.1 *The Early Bronze Age in Jordan*

The Early Bronze Age (EBA) in Jordan (3600 BCE – 2000 BCE), is marked by significant expansion of population, agricultural developments, and urbanization (Phillip 2008; Chesson 2007). This timespan has been divided into five periods, the EBA IA (3600 -3300 BCE), EBA IB (3300 -3000 BCE), EBA II (3000 -2750 BCE), EBA III (2750 – 2350/2300BCE), and the EBA IV (2350/2300 -2000 BCE) (Phillip 2008; Palumbo 2008). Each period has defining characteristics for its architecture, pottery, burial practices, and settlement patterns. The EBA IA is characterized by a more nomadic lifestyle, small permanent settlement structures and villages, and secondary burials in shaft tombs of multiple individuals. Pottery from the EBAIA has simple forms and construction, with bowls and jars with an orange wash and thumb imprints dominating the material culture (Adams 2002; Shaub 2009; Phillip 2008). The EBA IB is known to have an increase in sedentism, with a variety of home structures beginning to appear. The small communities had evidence of planned urbanization and fortified towns characterized as pre-political developments (Phillip 2008; Chesson and Goodale 2014). Urban areas like Jabal al-Mutawaaq in Southern Jordan the begin to enclose domestic structures within walled areas, whereas more rural areas like Tell Shuna in the North Jordan Valley still saw open towns and freestanding homes. Interestingly, these sites showcase there was no single style for homes in the EBA IB, but rather a collection of styles. These styles became more homogenized the smaller the settlement was, with rural areas having standardised structures and urban areas showing unique and potentially protected and specialised structures (Phillip 2008). Burial practices began to expand in the EBA IB period with primary and secondary burials in shaft tombs and charnel houses, such as those documented in Bab edh-Dhra', both capable of holding multiple

individuals in one location. Pottery resembles the EBA IA period, with simple shapes and construction of bowls and jars. New styles were emerging through this time with different vessel shapes, regional styles, and new fabric and temper incorporations as well (Chesson 2001; Haron and Clark 2022). The EBA II and III saw another increase in sedentism with the occupation site size and walled settlement structures and urban areas (Chesson 2001). Rectilinear homes were most common with multiple different rooms made from locally available materials. Homes contained multiple hearth structures throughout, and were organized on alleyways throughout the town (Phillip 2008). Burial practices continued to be observed in charnel houses, with both primary and secondary articulated burials still taking place. In the latter half of the EBA II and the EBA III, cremation and secondary burials of individuals became more common. Burial material consisted of pottery from local areas in the early EBA II, and spread to nonlocal items in the late EBA II and the EBA III. The early EBA II both periods had evidence of beads and pendants as burial goods as well. The later EBA II and the EBA III saw an increase in burial goods associated with jewellery costume items, with shells and bracelets also making an appearance. Weapons were also introduced into the burial chamber during this time (Chesson 2001; Phillip 2008). Pottery was developing faster, with complex technology in both vessel forms and decorations. Some areas like Bab edh-Dhra and Numayra had developed their own regional style as well throughout the EBA III. Wide rimmed and thick rimmed bowls were common, as well as four spout shallow bowl lamps. Some higher vessels included larger jugs with no distinguishable necks were seen in Bab edh-Dhra and Numayra (Haron and Clark 2022). The final 300 years of the Early Bronze Age, the EBA IV, reverts to some of the practices seen in the EBA IA and EBA IB. Urban centres began to be overshadowed it the preferred smaller sedentary occupation, and burial customs reverted to the simple shaft tombs with secondary

burials. Burial goods were also limited in this time, with pottery and beads or pendants making the majority of the material culture found (Chesson 2001; Phillip 2008). Contrary to burial practices and settlement patterns, the pottery of the EBA IV remained complex. Regional variation was seen in the type and pattern of slips used on pottery, and new forms like platters, cups, and teapots were introduced (Haron and Clark 2022).

2.1.1 *Wadi Faynan 100*

Located in the south of Jordan, Wadi Faynan 100 (*Figure 1*) was discovered in 1994 by H. Barnes and colleagues, and dated to the EBA IB (3300 – 3000BCE) (Adams et al. 2017; Wright et al. 1998). The Wadi Faynan 100 archaeological site is roughly trapezoidal in shape, measuring 11 hectares in size (Wright et al 1998). Wadi Faynan 100 has a dry and hot landscape, such that, during the dry months of the year, erosion of the landscape contributes to the discovery of artifacts like pottery. During the wet months of the year, the Wadi Dana, north of Wadi Faynan, floods, sending runoff through Wadi Faynan. The water then reshapes the landscape, allowing for archaeological material to be covered or discovered (Barker et al. 2007). These geological processes can lead to the discovery of artifacts, and can increase looting activity and can destroy archaeological significance (Adams et al. 2019). Human remains have been found in the southern area of Wadi Faynan 100, and have been subject to looting activities due the relative ease of spotting large burial structures in the landscape. Wadi Faynan 100 has been the focus of excavations lead by Dr. Katherine Wright and colleagues (1998), and Drs. Russell Adams, Alexis Dolphin, and colleagues since 2019 as part of the Barqa Landscape Project (BLP). The BLP excavations are working to determine the effects of metallurgic practices on the health of Early Bronze Age populations (Adams et al. 2019; Adams et al. 2023).

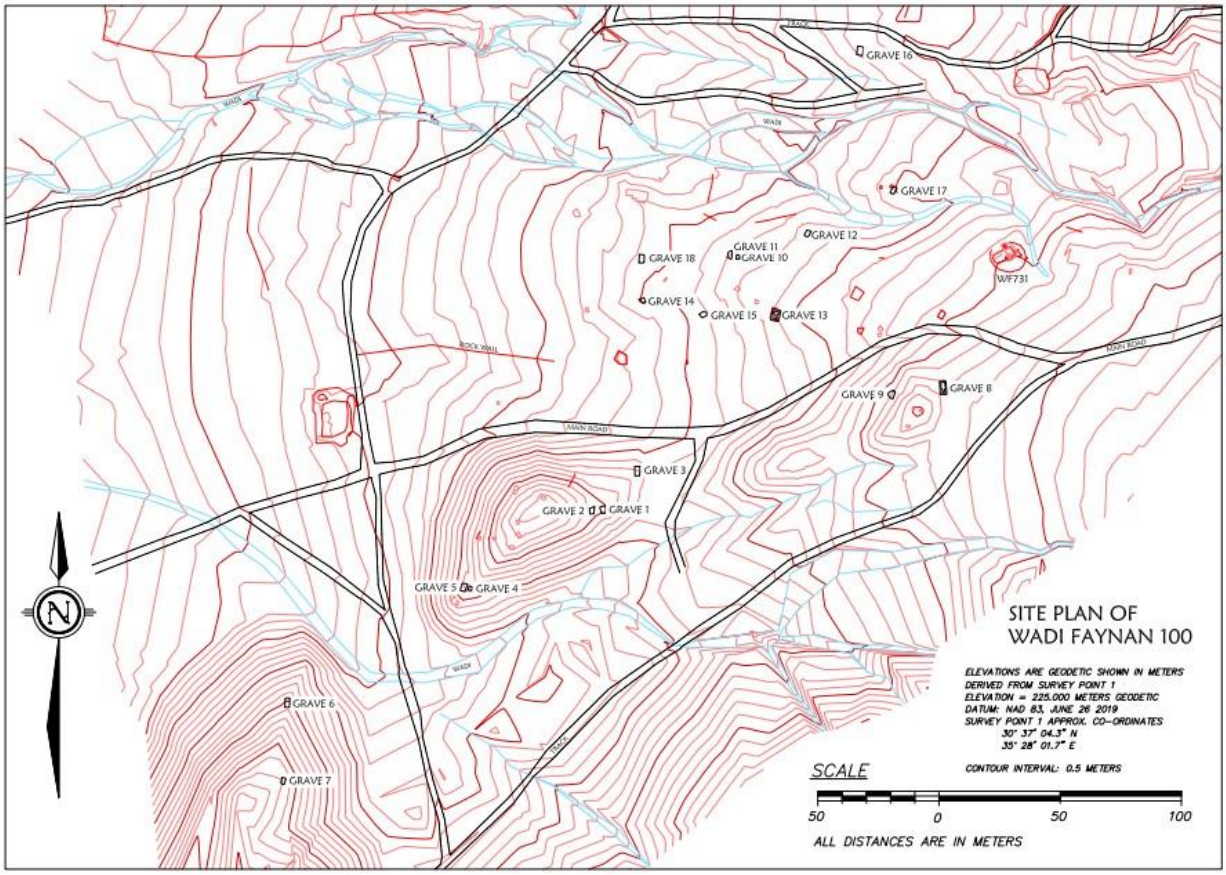


Figure 1. Wadi Faynan 100 site plan (Adams et al. 2023, pg. 1)

2.1.2 *Burials at Wadi Faynan 100*

EBAIA and IB grave structures vary in form. The EBA IB was a transitional time marked by a shift from a semi-nomadic lifestyle to a sedentary lifestyle (Chesson 2001, Sheridan et al 2014). Scholars suggest that these shifts may have been a result of the increase in population density, which in turn led to new burial structures and locations. Interment practices could vary from placement of a single body within a shaft tomb or dolmen, to the accumulation of multiple skeletons in charnel houses over successive phases of the Early bronze Age (Chesson 1999). Subadults were found with adult males and females in all types of tombs, surrounded by grave goods typical of the time period (Chesson 2001; Ortner and Frolich 2007; Rast and Shaub 1981). Grave goods were present throughout all phases of EBA occupation, ranging from simple clay beads to later inclusion of gold and silver. Wealthier assemblages are assumed to be of

individuals of higher power or importance while lower-status individuals received clay jugs, textile tools, and weapons (Phillip 2008; Chesson 2001; Al-Shorman and Khwaileh 2011).

However, at Wadi Faynan 100, a very different style of burial structure has been documented. This thesis research will focus on Grave 6 (*Figure 2, Figure 3*) of the Wadi Faynan 100 cemetery. In Wadi Faynan 100, Grave 6 was a charnel house that measured 4.2 metres long and 3.2 metres wide. Charnel houses were not used as the principal burial structure until the EBA II-III, making this a unique structure for the EBA IB (Chesson 2001). The deepest the grave reached was 80 centimeters, with evidence of 2 mudbrick collapses happening during its use.

Grave 6 in Wadi Faynan 100 has been subject to mild looting but has remained mostly intact (Adams et al. 2023). This grave was found to hold individuals who died from infancy to adulthood. Six loci were assigned to this grave, each one varying in matrix, depth, and amount of human remains and material culture recovered. Locus 1 was allotted to the looting and back dirt of this grave, with associated fragments of subadult and adult remains, beads, and pottery (Adams et al. 2023). Locus 2, located in the southern end of Grave 6, was only 1 cm deep and contained 3 white beads, 2 red beads, and 1 lambis bead. Locus 2 did not contain any bone. Locus 3 spanned the entire Grave length containing large numbers of snail shells and human bone (Adams et al. 2023). The matrix was debris from a mudbrick collapse, cementing the remains and making their removal from Grave 6 more difficult. Locus 4 was located in the northern end of the grave, had no human remains and was 3 cm thick. This locus ran underneath Locus 3 for approximately 1 metre south of the doorway. Nothing of note was found in this locus (Adams et al 2023). Locus 5 was another mudbrick collapse containing human remains spanning the entire grave. An articulated foot and spine were found in this locus, alongside relatively complete mandibles and crania (Adams et al. 2023). Locus 6, a deep rectangular area situated

between and beneath two white stone interior walls had a fine gravel and sand matrix. This locus contained well-preserved bones, including four vertebrae found within the matrix between these interior walls, articulated with a congenital abnormality. Additionally, Locus 6 contained 60 beads and 2 white clam shells (Adams et al. 2023). Overall, Grave 6 produced 78 bags of human bone that will be used in this thesis.

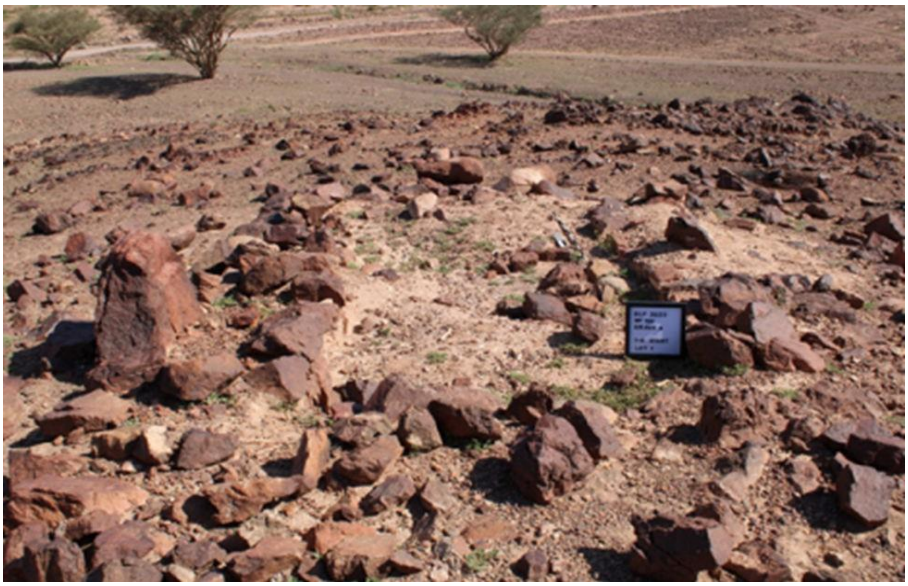


Figure 2. Grave 6 opening facing north (Adams et al. 2023, pg. 5)



Figure 3. Grave 6 closing facing south (Adams et al. 2023, pg. 5)

2.2 *Previous Research with Human Remains from WF100*

While Wright and colleagues carried out the first excavations at WF100 in 1997, the 2019 excavations by the BLP were the first to focus on burials at WF100 and the human remains interred within. These remains have been the subject of Masters thesis research conducted by graduate students in the Department of Anthropology at the University of Waterloo, covering a wide range of topics like trauma pattern analysis (Vieira et al. 2025), heavy metal pollution (Tan et al. 2022; Ruddell et al. 2025), dental anthropology (Tucciarone et al. 2020) and osteological studies (DiBiase et al. 2021). My thesis will contribute to this growing library of studies to provide more information on the number of subadult individuals at Wadi Fayan 100 cemetery in the Early Bronze Age.

Chapter 3: Minimum Number of Individuals (MNI) Methods

3.1 *Traditional MNI (White 1953)*

The calculation of a MNI estimate involves determining the hypothetical minimum number of individuals that could be present in a recovered assemblage (White and Folkens 2005). The most widely accepted method for MNI estimates comes from White in 1953. To apply this method, a researcher counts the left- and right- sided skeletal elements present, then uses the greater number as the estimate for the minimum number of individuals present (White 1953; White and Folkens 2005). For example, in a hypothetical situation there is a left parietal squama present, a left ulna, a left femur and right humerus. Because there is no repetition of side or type of bone, it is possible this could be from a single individual resulting in an MNI of 1. White's method solely estimates the lowest number of individuals possible in a collection, giving the researcher some idea of who could be represented, however, this is not a conclusive answer. When working with commingled remains, the fragmentary nature complicates the assessment, as elements might not articulate and the same bone may be counted multiple times, greatly exaggerating the estimated number of individuals (Lambacher et al. 2016; Palmiotto et al. 2019). This is a large reason why White's method is not a great fit for the collection from Grave 6. The identification of fragmentary subadult remains from varying life stages is a difficult task, and MNI estimates can easily be overestimated (Lewis 2007). White's method would exaggerate the estimated minimum number of individuals present and provide unreliable data.

To showcase the effectiveness of White's MNI method, a case study was performed by Vaduveskovic and Djuric (2019) on Bosnian war victims mass burial sites from 1995. Hailing from 5 different grave sites in Srebrenica, the graves were secondary in nature with a high degree of commingling from heavy machinery. Skeletal remains were catalogued in a couple of different

ways. A bone was recorded if it was at least 75% complete, if the bone was distinguishable or was articulated with another bone, or as a general body part for isolated skeletal remains (Vaduveskovic and Djuric 2019). After these observations were recorded, DNA testing was conducted to provide a 'correct' MNI based on known and missing individuals. The DNA MNI estimate was used as the true number of individuals and was compared to the MNI estimates found using White's method, to better understand the rate of error Whites' method can cause. Of all 5 graves studied, the lowest amount of error was of 56 individuals from the first grave site Snagovo 04. This was determined by comparing the estimated traditional MNI of 104 from the distal third of the right tibia to the DNA of 160 unique individuals buried. This resulted in an estimated error rate of 35%. The largest error was over 1000 individuals from one grave site, Cancari road 06. The original MNI using the traditional method was thought to be 203, while DNA testing revealed 1245 unique individuals were present (an estimated error rate of 83%). Vaduveskovic and Djuric note that the total number of unique identities from all graves does not represent the number of individuals buried there, as some individuals are represented multiple times from different sites (Vaduveskovic and Djuric 2019). The inaccuracy of traditional MNI estimates on commingled and fragmentary remains increases with the degree of disarticulation and/or breakage; implying that the more incomplete skeletal remains are, the poorer the accuracy of the MNI estimate becomes. It should be noted that the traditional method of MNI is not to find the exact number of individuals, but to provide a minimum. However, within this case study it is clear this method is not made to represent commingled remains. The massive error rates seen within these identifications greatly underestimate the number of individuals interred. This case study is one of the main examples as to why my thesis research will not use the traditional

approach. There is too much error for any estimate to be an accurate assessment of who could be buried at Grave 6.

3.2 *Zonation Method*

The complications of using the traditional MNI method on large and commingled collections have made way for new MNI methods to appear, like the Zonation Method from Knüsel and Outram (2004). The Zonation method was developed as an adaptation of the 1988 Dobney and Rielly method for faunal remains (Knüsel and Outram 2004; Dobney and Rielly 1989). The Zonation method breaks the human skeletal system into individual bones and assigns areas or "zones" with important and distinguishable elements for every bone. For example, Figure 4 shows a left humerus divided into its 11 "zones". Each zone has a description of where it is located and what features are located within it. To calculate an MNI estimate with this method, all bones found are catalogued with what zones are present (partial or not), what element it originated from, and what side of the body the bone is on (Knüsel and Outram 2004). This is done for all elements found, and all data are then interpreted like the traditional MNI methods such that overlapping sections of zone and side would be interpreted as having derived from two individuals. The Zonation method was developed specifically for fragmentary collections, enabling researchers dealing with such assemblages may be able to implement a reliable MNI method (Knüsel and Outram 2004; Dobney and Rielly 1989). However, this method has been criticized for double counting individuals, its reliance on complete bones, and producing biased estimates with smaller samples (Lambacher et al. 2016). Applying this method to a commingled and fragmentary subadult assemblage would increase the risk of depending on complete elements and outputting biased results.

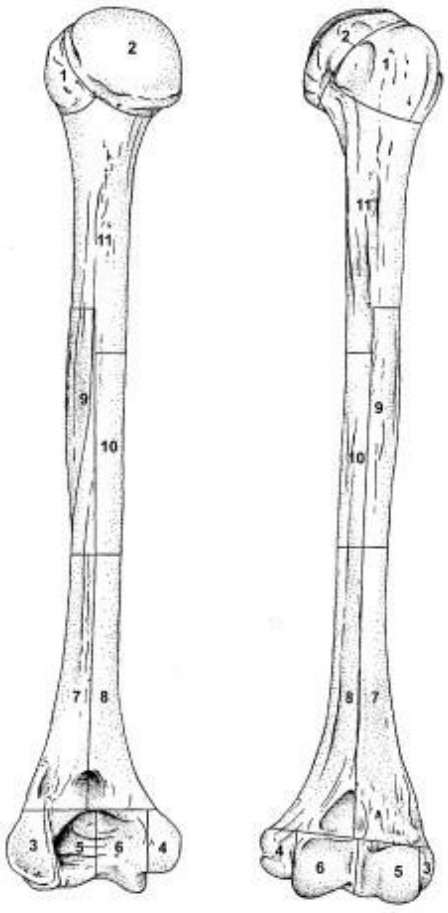


Figure 4. Left Humerus, posterior and anterior views with codified zones (Knüsel and Outram, 2004, pg 90).

The Zonation method's effectiveness was tested by Palmiotto and colleagues (2019) on the collection of the USS *Oklahoma* Pearl Harbour attack victims – with an original sample size count of 394 individuals. Prior to analysis, all elements were recorded once again for accuracy. The collection was mostly intact and did not have a large amount of fragmentation. The study concluded that the Zonation method was able to identify 364 individuals through cranium zones, 343 individuals through femoral zones, and 292 individuals through right humeri zones. Compared to the other MNI methods used (MLNI [Most Likely Number of Individuals], MNI by mtDNA [Minimum number of individuals by mitochondrial DNA], and GMT [Grand Minimum

Total]), the Zonation MNI estimates were conservative. Palmiotto and colleagues attributed this to the lack of fragmentation in the collection (Palmiotto et al. 2019). Despite this, the Zonation method provided better results than the traditional MNI and MNE methods. Palmiotto and colleagues concluded the Zonation method is useful, inexpensive, and provides a clear standardized identification system, which is useful in forensic and archaeological applications (Palmiotto et al. 2019). This method does provide its strengths and is quite similar to the Landmark System, however was not chosen because of the criticisms by Lambacher and colleagues.

3.3 *Landmark System*

A third method of MNI analysis is the Landmark System. Developed by Mack et al. in 2015, this method addresses the issues with estimating an MNI for fragmentary and commingled remains. Taking inspiration from the Zonation method, the Landmark System separates each bone into significant landmark sections. Each landmark can be identified based on completeness to develop an MNI estimate. Landmarks are selected based on the standard skeletal anatomy taught from various textbooks (Mack et al. 2015). Specific landmarks are chosen by their relative continuity across individuals, such as auricular surfaces and tubercles. Other sections of bone such as shafts or clearly defined sections are included as well. A bone can have a landmark count from 3-15, depending on the number of distinguishable landmarks. To apply this method, human skeletal elements are examined for specific landmarks (i.e. the greater trochanter of a femur), and the side of the body the landmark is from is also recorded. These observations are then interpreted like the traditional MNI method, where any repeated landmark and side is counted as one individual. A complete collection of the Landmark System for an adult skeleton is offered through supplementary information on the online Wiley library. The only landmarks cited in the

publication are of a right scapula (*Figure 5*), while all other codified bones are found through downloadable files underneath the publication. No such reference exists for subadult skeletons; therefore, significant work was required to adapt this method for use with subadult skeletons in this thesis. I believe this method is the best approach for addressing my research question as it allows for a realistic approach given the time frame of my research while also efficiently addressing an MNI estimate.

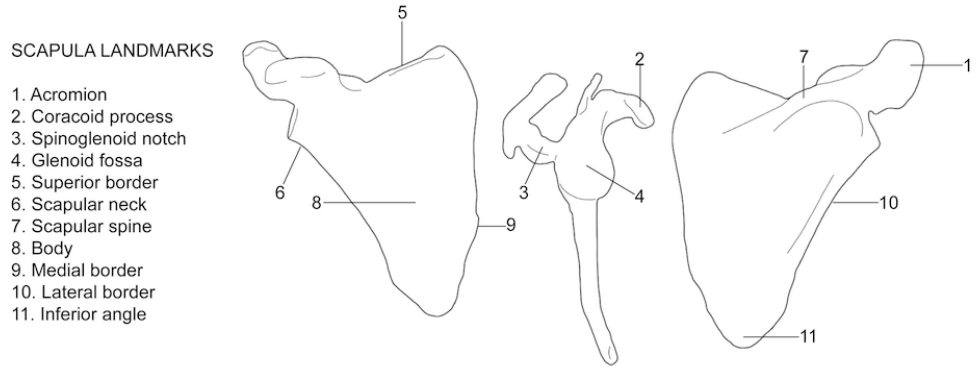


Figure 5. Right scapula, anterior, lateral, and posterior views, with codified landmarks (Mack et al., 2015, pg 4).

The original study to develop this method by Mack et al. (2015) analyzed commingled burials from Bolores, Portugal. This study recovered 5773 skeletal fragments, of which 4765 were able to be identified, and 1008 fragments being identified as indeterminate or simply as long bones. The remains were originally identified in the field with basic techniques that were further refined at the University of Iowa. Remains were identified by element, side, age-at-death (subadult or adult), and sex, whenever possible. Due to the varying ages of bone fusion, Mack and colleagues acknowledged that some error might be present in the identification of adult and subadult remains. After the basic inventory was completed, the Landmark System was applied to all identifiable bones. Landmarks were identified as being present if more than 50 percent of the

landmark was intact/visible. Once all landmarks were accounted for, the largest sum of the landmarks examined were used to produce an MNI count. Multiple counts were taken to establish an average, with counts being used from cranial elements, the axis, the atlas, the os coxae, clavicle, scapula, patella, talus, calcaneus, metacarpals, metatarsals, and long bones. Finally, the MNI was recounted by examining these groups again, noting any unique characteristics to receive a final estimate. Mack and colleagues recognized the MNI to be best showcased through dental remains as they survive best in inhumation, however, they did also suggest the use of other skeletal elements as well. The use of zooarchaeological methods to determine MNI in human remains provides several benefits. This method of identification is fast, can offer an understanding of the site itself, and can help researchers understand taphonomic forces within the burial. This in turn can glean more information regarding mortuary practices at this site, and the people who occupied it (Mack et al. 2015). The Landmark System is ideal for producing an MNI estimate for Grave 6 given that it is highly fragmentary and commingled. This method gives the option to separate known fragments from unknown and analyze both groups. As MNI estimates are an important first step for research at a site, the Landmark System will be able to provide the most confident estimate.

Speaking further on the Landmark System, a study done by Lambacher et al. (2016) evaluated 3 MNI techniques in a commingled and fragmentary collection. They compared the use of the traditional MNI from White, the Zonation system, and the Landmark System. It was shown that not only did the Landmark System outperform both methods, but that the Landmark System is well suited to fragmentary collections as it can divide any bone into digestible fragments (Lambacher et al. 2016). Alongside this, the Landmark System reduces the likelihood to double count individuals, allowing a conservative minimum estimate to be achieved.

3.4 *Age-at-Death (AAD) Methods*

Age-at-Death (AAD) is the approximate age of the individual when they died. The estimation of AAD is an important step for subadult identification, not only to determine if the remains are in fact subadults, but to determine which the skeletal elements have developed. The younger a child is, the smaller an age range is, due to their rapid development (Schaefer et al. 2009). Age estimation does not have one specific method, but rather a compilation of methods from various researchers based on specific populations (Schaefer et al. 2009). Because of this, it is important to note some error will always be present, particularly since most age estimation methods may not reflect the biological and developmental patterns of the Early Bronze Age Jordan populations. For this research, such discrepancies could influence the accuracy of age-at-death estimates, which in turn may affect the interpretation of subadult health and growth at WF100. Methods are focused on measurements of bone, size comparison, and the presence of certain characteristics or landmarks. AAD was performed as age is an important factor for subadult MNI estimation. These estimations are typically based on using the highest number of occurring element from one side (i.e. the left femur), but when considering the use of commingled and fragmentary remains, the inclusion of as much data as possible is necessary. Taking direction from Osterholtz and colleagues, they state the MNI will likely include multiple skeletal elements and age groups (Osterholtz et al. 2014). I found this to be true and did not want to risk inflating the MNI estimate due to an inclusion of bones that could have overlapping age ranges and be from one individual. Therefore, the AAD inclusion can combat this by decreasing the number of repeated bones of one age.

Required knowledge of subadult bone development is necessary to best identify the subadults from the adults for age-at-death estimates and MNI estimates. In order to accurately assess this

collection, one must be able to understand how bone develops, what bones fuse together and where, and be able to identify what fusing bone looks like.

The development of bone is known as ossification, or osteogenesis. This process begins at around 6 weeks gestation and ends around age 25 (National Cancer Institute 2025). There are two forms of bone development known as intramembranous and endochondral, where the former refers to cranial bone and clavicle development and the latter refers to development of all other bones (National Cancer Institute 2025; Uhl 2013). Endochondral bone growth creates the structure of the bone from a cartilage model, then slowly ossifies throughout a child's development (National Cancer Institute 2025). Figure 6 provides a visual reference of these models of bone growth. Intramembranous bone growth creates bone by developing ossification centres that grow outwards, slowly forming the final bone shape (National Cancer Institute 2025; Lewis 2007). Refer to Figure 7 for a visual reference.

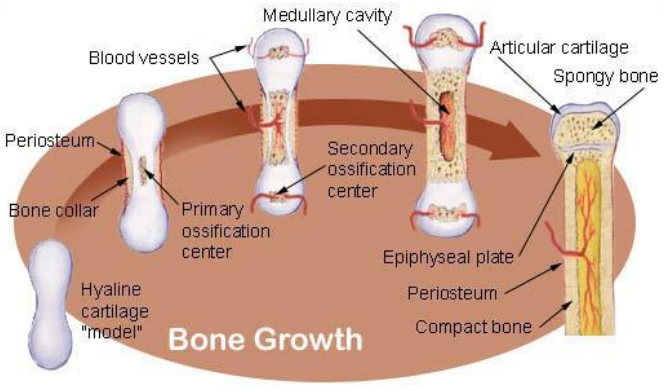


Figure 6. Endochondral bone growth model. (Wikimedia Commons, 2025).

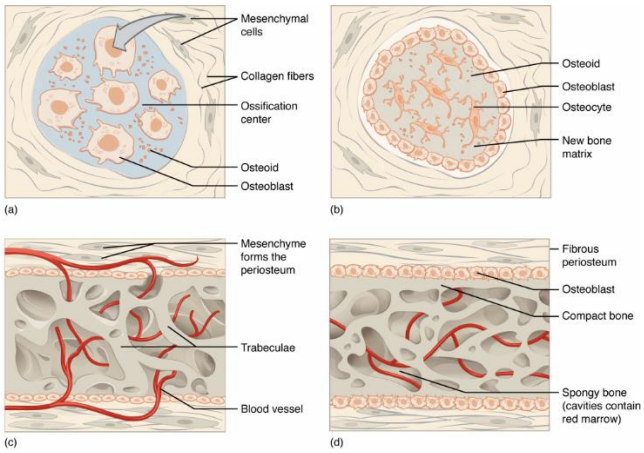


Figure 7. Intramembranous bone development model. (Carstens, 2023, pg 339).

For the individuals found in Grave 6, the Landmark System was an easy task to produce AAD estimates due to its reliance on comparison of certain landmarks found throughout the development of bone. If an element required for estimating AAD was missing it was deemed indeterminate. The ability to determine AAD often was determined by the completeness of elements found, as most often fragile or thinner sections required for an age estimate (i.e. the ramus or convex border of an ischium) were missing or severely damaged.

3.5 *Landmark Modification for Subadults*

To use the Landmark System in this thesis, modifications were needed to make it applicable to subadult remains. Modifications to the adult Landmark System have been performed by Bourgeois and colleagues (2021), however, no modifications have been made to fit subadults specifically (Bourgeois et al. 2021). Because of this, the subadult Landmark System involved: 1) developing standard images for identification of subadult landmarks on bone; the subadult skeleton and each bone's morphology, including epiphyses; 2) identifying each subadult bone, including epiphyses, and providing estimates of age-at-death for each bone; 3) estimation of MNI using the subadult Landmark System; and 4) refining MNI estimates using age-at-death

estimates. In addition, every bone and identifiable landmark was drawn using the Krita Digital Painting Software, a Wacom Intuos Draw CTL-460 drawing tablet, Microsoft Word, and Microsoft Photos Editing Feature. Reference images for the *pars basilaris*, *pars lateralis*, temporal, centrum and neural arch of a vertebra, scapula, clavicle, sternum, humerus, ulna, radius, ilium, ischium, pubis, the second metacarpal, phalanges of the hand, all carpals, femur, tibia, fibula, patella, all tarsals, the second metatarsal, and the phalanges of the foot were taken from Baker et al.'s *The Osteology of Infants and Children* (2005), scanned into a PDF document, uploaded into Krita, and traced. The vertebrae, second metacarpal, and second metatarsal were used for general morphology referencing. No metacarpals or metatarsals were identified beyond 'metacarpal' or 'metatarsal'. Vertebrae were identified into cervical, thoracic, or lumbar when possible, using the correlating reference images from *The Osteology of Infants and Children* (2005). Details were added based on the PDF scans and subadult Bone Clone models used in the University of Waterloo Bioanthropology Lab. Small facial bones were omitted from this study once an inventory was taken, as very few were found in the collection with recognizable landmarks to be analyzed. All landmark images created can be found in Appendix A.

Because the WF100 collection had not been sorted previously, I was first tasked with organizing the 78 bags of commingled human remains before focusing on the subadult material. This process was carried out by myself, the lab manager Jeff Coffin, and incoming graduate student, and two graduate students in my cohort. Each bag was emptied, and its contents were sorted into identifiable human remains, unidentifiable fragments, faunal remains, and subadult remains. Identifiable adult elements were recorded in a shared Excel spreadsheet and repackaged by skeletal region (e.g., long bones, vertebrae, scapulae, ribs and clavicles, and hand and foot bones). Subadult elements were separated into their own bags for later detailed analysis. Once

sorting was complete, all material was transferred into thick plastic bags labeled with the corresponding locus and paper bag number. I then conducted a second round of analysis on the subadult remains, identifying each element as thoroughly as possible. These identifications were entered into a separate Excel spreadsheet that tracked the element type, if it could be used to determine an MNI estimate or an AAD estimate and what anatomical landmarks were present on the element identified. This was organized on the Excel spreadsheet by its corresponding plastic bag, locus number, and grave number. Once all elements were identified, subadult bone was placed back in its corresponding bag for storage. Once all data was input, certain elements were taken out of storage to photograph using my personal cellphone.

Chapter 4: Materials

4.1 *The Assemblage*

When choosing a sample of subadult bones from the Grave 6 assemblage multiple factors were considered, including damage to the bone, amount of bone available for age-at-death estimation, and presence or absence of detectable landmarks. A total of 984 subadult bones were collected across all 6 loci, with 439 being suitable for analysis, approximately 45% of the found assemblage. A bone was considered suitable for analysis if at least 25% of the bone was present or had recognizable landmarks. An example of this would be if approximately 25% of a femoral shaft was identified by the linea aspera, it could be included. If a long bone shaft was found, but could not be identified as belonging to a specific bone, it was omitted. Not all bones that are represented in this sample could be assigned an estimated age-at-death, but they are included for the purposes of calculating MNI estimates. Due to the use of the Landmark System for estimating MNI, the typical 50% of bone used to determine MNI was not followed (Mack et al. 2015). Below outlines the specifics for each type of bone, and how it was determined to be included in this study.

4.1.1 *Long bones*

Long bone epiphyses were used if there was at least 25% of the bone or identifiable sections, such as the lateral or medial condyle of a distal femur epiphysis. The same is true for long bone shafts and broken epiphyses. If zero identifiable landmarks were present, these bones were not used for MNI or age-at-death estimations. In total 175 long bones were identified and 99 were used in MNI calculations, making 56% of the sample usable in this research. The most common bone found was the femur, and the long bones were typically in poor condition, with shafts split open and damaged or missing bone present on most of the epiphyseal surfaces.

4.1.2 *Cranial Bones*

Cranial bones were used sparingly due to the inability to age and identify squamous portions within this sample. Smaller cranial bones such as the *pars lateralis* and *pars basilaris*, provide higher confidence when estimating age-at-death and MNI, but have limited capacity to provide accurate ages past gestation (Fazekas and Kosa 1978). If damage was minimal to these bones, they were included in age-at-death estimates and MNI estimates. Therefore, cranial bones were identified within the larger sample, but were used sparingly for AAD estimation due to the uncertainty of age ranges. In total, 91 cranial bones were found and 9 were included in MNI calculations, 9% of the sample found. This was because the majority of cranial bones found were small flat sections of the cranium. The most common cranial bone found was hard to determine as identifiable landmarks were rare and were in poor condition. Breaks and splintering were found throughout these bones, with some crumbling after they were picked up.

4.1.3 *Irregular Bones, Flat Bones*, and *Vertebral Elements*

Irregular and flat bones include all bones within the pectoral girdle, pelvic girdle, and the patella (Fazekas and Kosa 1978). Ribs were not used as size and maturity levels are difficult to determine (Fazekas and Kosa 1978). The manubrium and sternum were used for both MNI and AAD but are not represented well within the assemblage. Reliable aging methods are not available for the ribs, manubria, and sternums, making it much harder to include them within the age-at-death estimation. The pelvic girdle was included entirely, as all bones represented have reliable age estimation methods. Patellae in this sample were examined when possible, however, it is difficult to estimate an age-at-death for these bones due to a lack of morphological changes, outside of size and robustness during their development. Preservation from this bone category was subpar, as many bones including ribs, clavicle, and scapulae were extremely damaged.

Luckily, because of the robust sections in the pelvic girdle, the robust borders of the scapulae, and patella, 132 elements were found, and 105, or 79%, were used. Most of the irregular and flat bones had recognizable landmarks despite their preservation that could be used for both MNI and AAD methodologies. Vertebral elements were in abundance within this collection and were represented in almost all age categories. To pick a sample of the vertebrae present, damage to the centrum and the amount of fusion to the neural arches were considered. If the centrum was too damaged to view the growth lines on a centrum, the vertebra was not considered. The same process was repeated if only neural arches were present. While there was an abundance of vertebrae, many of the elements found could not be identified into cervical, thoracic, or lumbar. Large chucks of exposed spongy bone with a distant 'C' shape on the outer border was the majority of this sample. When it was possible, the type of vertebra was identified and included within the sample. One hundred and forty-six vertebral elements were found and 105, meaning 71% of the sample was used.

4.1.4 *Hand, Wrist, Foot, and Ankle Bones*

Hand, wrist, foot and ankle bones were the best-preserved bones within the assemblage. These bones are more difficult to provide an age-at-death estimate for, but easy to identify. Because of this dilemma, all bones within this category were represented with a large age range, with an exception for the talus and calcaneus, for which a more concise age estimate could be achieved (Fazekas and Kosa 1978). Long bones within the hands and feet were identified based upon the presence or absence of fused epiphyses. Metacarpals and metatarsals were identified as such, however, determining their exact position, like an M1 or M4 was not possible due to the damage. Often times the metacarpal was broken in half and damaged on the proximal epiphysis. Proximal, medial, and distal phalanges were not separated because of this issue as well. Proper

identification was difficult given the time frame due to the lack of epiphyses found fused together with the shafts of metatarsals, metacarpals, and phalanges. The condition of these bones ranged from near perfect condition with complete facets to extremely damaged and barely recognizable. Figures 66 to 69 in Appendix B showcase the condition these elements were in. One hundred and sixty bones were identified, and 126, or 78%, were used for the MNI estimate, because of their condition and lack of reliable age estimation techniques.

4.2 *Estimation of Age-at-Death*

AAD, or the Age-at-Death, was estimated using several methodologies from researchers found in *Juvenile Osteology: A Laboratory and Field Manual* (Schaefer et al. 2009). The sacrum, radius, ulna, innominate bone (complete), tibia, fibula, and foot were estimated using data from Coimbra, Portugal inhabitants born between 1904 and 1938 from ages 7-29 years old (Coqueugniot and Weaver 2007). The sternum, humerus, femur, and fibula were estimated from the male Bosnian war dead in 1995 (Schaefer 2008). The clavicle estimation came from 19th century English and 20th century Portuguese remains (Black and Scheuer 1996). The scapula was estimated using data from the Scheuer collection in the University of Dundee, containing both documented and undocumented remains (Rissech and Black 2007). The ilium was estimated using data from documented 18th and 19th century remains originated in Spitalfields, London (Molleson and Cox 1993). The ilium was estimated using data from autopsies of multiracial Americans from 1977 to 1979 (Webb and Suchey 1985). Further information for the tibia and fibula was gathered from Portuguese individuals buried between 1903 and 1975 (Cardoso 2008). The *pars lateralis* and *pars basilaris* were estimated using data from 20th century Hungarian fetal autopsy remains (Fazekas and Kosa 1978). Some images were used from *The Osteology of Infants and Children* (2005) for references of epiphyseal union, bone formation, and bone size of

the femur, tibia, fibula, metacarpals, metatarsals and phalanges of both the hand and foot (Baker, Dupras, and Tocheri 2005).

Multiple methods and standards were consulted to ensure there was an adequate age range given to each element, as determining an age-at-death from one population may result in higher error margins. Although combining methods has the potential to provide compound error, in this study the results from different methods were highly consistent, producing similar averages and in some cases identical. This overlap indicates the risk of compounding error was minimal, while still incorporating standards from different populations. To take a conservative approach, the highest and lowest age estimates were used in the ranges given. One example of this would be from the calcaneus epiphysis. Referenced from Schaefer et al. (2009) and Baker et al. (2005), the calcaneus epiphysis can begin fusion from 10 years in females, and 11 years in males, and fusion is complete from 16 years in a female to 20 years in a male. To incorporate all possible outcomes of this fusion timing, a range of 10-20 years was given to all epiphyses found.

AAD estimation of the individuals found in Grave 6 was relatively straight forward due to its reliance on comparison of certain landmarks present throughout the development of bone. If an element was unavailable for the purposes of estimating the age-at-death, the age of that element was designated as ‘undetermined’.

Chapter 5: Results

5.1 *Minimum Number of Individuals (MNI)*

Represented in the tables below are the subadult human bones that could be positively identified in Grave 6, Locus 1. Thirteen subadult bones were found within Locus 1, and 5 bones were identifiable. Of all elements studied, one cranial element (a mandible) was found. Moving lower within the body, the arches and centre of 1 thoracic vertebra were found. Only 1 distal phalanx and 1 distal phalanx epiphysis were found. The final bone that could be identified within Locus 1 was a proximal epiphysis of a femur. Unfortunately, this epiphysis was too small and too damaged to be sided. Within all of Grave 6, Locus 1, the MNI is 1 as these bones could have been from one individual.

Context	Skeletal Section	Element	N	Side
Grave 6, Locus 1	Subadult Cranial Elements	Mandible	1	N/A
	Subadult Vertebral Column	Thoracic vertebra - arches and centrum	1	N/A
	Subadult Hand/Foot	Distal phalanx	1	N/A
		Distal phalanx epiphysis	1	N/A
	Subadult Lower Limb	Femur – proximal epiphysis	1	N/A
Total Number of Elements			5	

Table 1. Grave 6, Locus 1 MNI Results. Sides are indicated as L (left), R (right), or N/A for unsided.

Below in Table 2 are the findings from Grave 6 Locus 2. Eleven subadult bones were found within this locus. The only recognizable fragments from the assemblage were a femoral neck and a small, almost complete right ischium. As this could have been from one individual, the MNI is estimated at 1.

Context	Skeletal Section	Element	N	Side
Grave 6, Locus 2	Subadult Pelvic Girdle	Ischium – ischium body	1	R
		Ischium – partial lunate surface	1	R
	Subadult Lower Limb	Femur – neck	1	N/A
Total Number of Elements			3	

Table 2. Grave 6, Locus 2 MNI Results, Sides are indicated as L (left), R (right), or N/A for unsided.

Table 3 represents the findings from Grave 6 Locus 3, one of the larger loci in this collection. Eighty-three subadult bones were found within this locus, with 23 elements being identifiable. This locus is representative of an MNI of 3 individuals. This estimation comes from the count of right femora, where 2 right proximal halves of a femur are present, and a third right femoral shaft of overlapping sections is represented.

Context	Skeletal Section	Element	N	Side
Grave 6, Locus 3	Subadult Cranial Elements	Pars Basilaris	1	N/A
	Subadult Hand/Foot	Phalanx/ Metacarpal/ Metatarsal	2	N/A
		Phalanx/ Metacarpal/ Metatarsal - epiphysis	2	N/A
		Talus	1	L
	Subadult Pelvic Girdle	Acetabulum	1	N/A
		Iliac epiphysis	1	N/A
	Subadult Lower Limb	Femur – proximal half	3	2 R, N/A
		Femur – head	2	N/A
		Femur – shaft	1	R
		Femur – distal epiphysis	3	N/A
		Patella	2	1 R, 1 L
		Tibia – distal epiphysis	1	R
		Tibia – proximal half	1	1 R, 1 N/A
		Tibia – proximal epiphysis	1	R
Total Number of Elements			23	

Table 3. Grave 6, Locus 3 MNI Results, Sides are indicated as L (left), R (right), or N/A for unsided.

In Locus 4, 1 subadult bone was found, but the element was not identifiable. Based on this knowledge, the MNI is 1 individual.

The largest of the loci, Locus 5, represents the majority of the collection from Wadi Faynan 100, Grave 6. This locus provides evidence to support a small number of children were buried together within this grave. With an estimated MNI of 7, this layer of Grave 6 contains the highest number of interred children in one section with 710 subadult bones found. Thirty-seven per cent of the bones, or 263 elements, were able to be identified. The MNI estimate was found using the left and right femora. All landmarks were divided into the left and right side and were recorded as a new or repeated occurrence on each side. By using this method, 7 right femora were identified using 3 whole femora, 1 right greater trochanter, 2 proximal halves of a right femur, and 1 right proximal end of a femur. Any other identifiable landmarks found on the right side of a femur can complete these 7 femora.

Context	**Skeletal Section**	**Element**	**N**	**Side**
Grave 6, Locus 5	Subadult Cranial	Pars Basilaris	2	N/A
		Pars Lateralis	4	2 R, 1 L, 2 N/A
	Subadult Vertebral Column	Thoracic Vertebra	3	N/A
		Vertebra – unclassified	89	N/A
		Vertebra – centrum	6	N/A
		Sacrum	6	N/A
	Subadult Upper Limb	Humerus	4	3 R, 1 N/A
		Humerus – distal shaft	2	2 N/A
		Humerus – distal epiphysis and shaft	1	L
		Humerus – proximal half	2	1 R, 1 L
		Humerus – head	3	1 R, 2 N/A
		Humerus – distal epiphysis	3	1 R, 2 N/A
		Radius	1	N/A
		Radius – proximal epiphysis	1	N/A
		Radius – shaft	3	1 L, 2 N/A
		Radius - distal epiphysis	1	L

Context	Skeletal Section	Element	N	Side
Grave 6, Locus 5	Subadult Upper Limb	Ulna – proximal half	1	R
		Ulna – distal epiphysis	3	2 R, 1 L
	Subadult Pectoral Girdle	Scapula	5	1 R, 1 L, 3 N/A
		Scapula – glenoid fossa	4	1 R, 1 L, 2 N/A
		Manubrium	1	N/A
		Clavicle	5	3 R, 2 L
		Clavicle - epiphysis	1	N/A
		Sternum	1	N/A
	Subadult Hand/Foot	Phalanx/ Metacarpal/ Metatarsal	31	N/A
		Phalanx Metacarpal/ Metatarsal -epiphysis	6	N/A
		2nd Cuneiform	1	N/A
		3rd Cuneiform	2	2 L
		Cuboid	2	1 R, 1 L
		Lunate	10	3 R, 4 L, 3 N/A
		Calcaneus	3	2 R, 1 L
		Calcaneus – epiphysis	5	N/A
		Navicular	1	N/A
	Subadult Pelvic Girdle	Os Coxa (Ilium and Ischium)	4	1 L, 3 N/A
		Acetabulum	2	N/A
		Pubis	2	2 L
		Ilium	2	N/A
		Ilium - iliac crest	1	N/A
		Ilium - iliac crest epiphysis	1	N/A
		Ilium - iliac wing	2	N/A
	Subadult Lower Limb	Femur	6	3 R, 2 L, 1 N/A
	Subadult Lower Limb	Femur – head	3	1 R, 2 N/A
		Femur – shaft	1	N/A
		Femur – greater trochanter	2	1 R, 1 N/A
		Femur – proximal half	3	2 R, 1 L
		Femur – proximal fragment	1	L
		Femur – distal half	2	1 R, 1 L

Context	Skeletal Section	Element	N	Side
Grave 6, Locus 5	Subadult Lower Limb	Femur – distal epiphysis	3	1 R, 1 L, 1 N/A
		Femur - medial condyle of distal epiphysis	3	1 L, 2 N/A
		Femur – lateral condyle of distal epiphysis	2	2 R
		Patella	2	2 L
		Tibia	2	1 R, 1 L
		Tibia – proximal epiphysis	2	1 R, 1 N/A
		Tibia – proximal half	1	L
		Tibia – distal half	1	L
		Tibia – distal epiphysis	2	2 L
		Fibula	1	R
		Fibula – shaft	1	N/A
Total Number of Elements			263	R

Table 4. Grave 6, Locus 5 MNI Results, Sides are indicated as L (left), R (right), or N/A for unsided.

In the final locus of Grave 6, Locus 6, 221 subadult bones were found, and 98 elements were identified. The femora of Locus 6 were used to determine the MNI by dividing the left and right femoral landmarks. There are 2 complete left femora and 1 left proximal half of a femur, thereby suggesting at least 3 individuals are represented in this sample.

Context	Skeletal Section	Element	N	Side
Grave 6, Locus 6	Subadult Cranial	Pars Basilaris	2	N/A
	Subadult Vertebral Column	Vertebra – unclassified	40	N/A
	Subadult Upper Limb	Humerus	2	1 R, 1 L
		Humerus – shaft	1	R
		Humerus – distal shaft	1	L
		Radius – proximal half	1	R
		Ulna – proximal epiphysis	1	R
		Ulna – proximal half	1	R
	Subadult Pectoral Girdle	Clavicle	2	1 L, 1 N/A
		Clavicle – medial epiphysis	1	N/A

Context	Skeletal Section	Element	N	Side
Grave 6, Locus 6	Subadult Pectoral Girdle	Scapula	2	N/A
	Subadult Hand/Foot	Phalanx/ Metacarpal/Metatarsal	20	N/A
		Phalanx Metacarpal/ Metatarsal – epiphysis	8	N/A
		Capitate	1	R
		Trapezoid	1	L
		Calcaneus	2	R
		Talus	2	R
	Subadult Pelvic Girdle	Ischium	1	N/A
	Subadult Lower Limb	Femur – proximal half	1	L
		Femur	5	1 R, 2 L, 2 N/A
		Femur – distal epiphysis	1	N/A
		Patella	1	L
		Ilium – iliac wing	1	N/A
Total Number of Elements			98	

Table 5. Grave 6, Locus 6 MNI Results, Sides are indicated as L (left), R (right), or N/A for unsided.

5.2 *Age-at-Death Estimates (AAD)*

Represented in the figures and tables below are the results of age-at-death estimations alongside a possible distribution of skeletal elements based on these estimates. These groupings were constructed for the purpose of refining the MNI, and illustrate how overlapping AAD estimations were evaluated in order to produce a conservative estimate. These groupings are interpretations and do not reflect the true number of subadults buried, nor do they represent confirmed anatomical associations of skeletal elements.

Skeletal elements were grouped based on a combination of anatomical compatibility, side, developmental stage, and their estimated age-at-death following the established practices for sorting commingled remains (Buikstra and Ubelaker 1994; Scheuer and Black 2016; Ubelaker

1989). Elements were only paired together when there was no overlap in side or skeletal region, and when the estimated age ranges were compatible (Adams and Konigsberg 2004). Paring elements to determine a revised estimate for MNI is used by Adams and Konigsberg for another technique – the Most Likely Number of Individuals (MLNI). This requires elements to be sided, an estimate of age-at-death to provided, and elements to be pair-matched based on similar morphology and age (Adams and Konigsberg 2004). Because elements in the WF100 collection were extremely fragmentary, bones could not be pair-matched by morphology, but were able to be pair-matched using age.

For example, a left femoral shaft and greater trochanter with an age-at-death estimate of 12–18 years was grouped with a right distal tibia epiphysis and a clavicle falling within the same age range, making sure there was no overlap with similar elements from the same side. A left femoral shaft and distal epiphysis present with an estimated range of 12-18 years was present as well. These two femora might be from one individual, but have no matching morphology to compare, therefore will be pair-matched based on age ranges alone. This was the best way to provide a conservative estimate for the minimum number of subadults represented by identifying sets of elements that could plausibly belong to the same individual based on developmental and anatomical markers that did not repeat. In more difficult situations—such as when multiple elements fell within similar age ranges but lacked an identifiable side —elements were grouped together to avoid overestimation. This resulted in the tables and figures below, where some individuals have rather large age ranges compared to others.

Locus 1

From Locus 1, the MNI calculations estimated that 1 individual was present. With inclusion of data found from AAD estimation, this number can be grouped to produce 2 individuals. One individual contains the proximal femoral epiphysis estimated to be 5-7 years old and a thoracic vertebra estimated to be 6-12 years old. The size of the femoral epiphysis was compared to a same-size image from the development of a femur, where it was found to be slightly larger than a 5-year-old femur, but had not developed a flattened lateral margin (Baker et al. 2005; Schaefer et al. 2009). According to the morphological summary of the femoral head found in *Juvenile Osteology* (2009), this feature typically develops by age 8; its absence suggests a maximum age-at-death estimate of 7 years old (Schaefer et al. 2009). A thoracic vertebra from the same locus was assigned an AAD range of 6-12 years old, while a mandible was estimated to be 10-13 years old (Albert and Maples 1995; Bagnell et al. 1977; Baker et al. 2005; Schaefer et al. 2009; Baker et al. 2005; Moorrees et al. 1963). The mandible is associated with a second individual as the estimated age-at-death range of 10-13 years old does not align with the femur of 5-7 years old. The distal phalanx and phalanx epiphysis are harder to classify due to the large estimated age range for these bones within the existing literature (Birkner 1978; Baker et al. 2005).

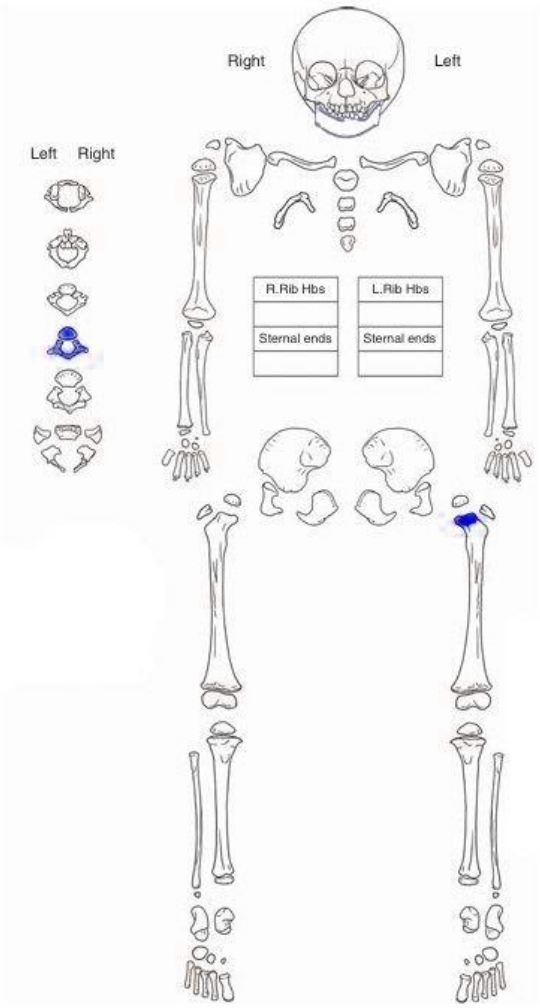


Figure 8. Skeletal elements from Grave 6, Locus 1 (estimated age range: 5–13 years), highlighted in blue. Elements may represent one or more subadults.

Context	Skeletal Section	Element	Side	Estimated Age-At-Death	Source
Grave 6, Locus 1	Subadult Vertebral Column	Thoracic Vertebrae	N/A	6-12 years old	Albert and Maples 1995; Bagnell et al. 1977; Baker et al. 2005; Schaefer et al. 2009
	Subadult Lower Limb	Femur – Proximal epiphysis	N/A	5-7 years old	Baker et al. 2005; Schaefer et al. 2009

Table 6. Skeletal elements from Grave 6, Locus 1 (estimated age range: 5-12). Sides are indicated as L (left), R (right), or N/A for unsided.

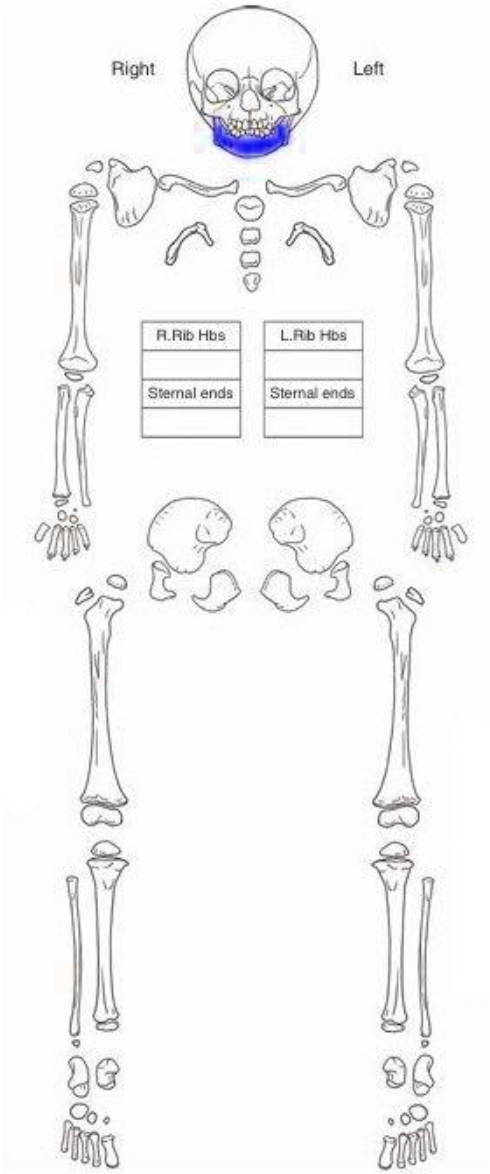


Figure 9. Skeletal elements from Grave 6, Locus 1 (estimated age range: 10–13 years), highlighted in blue. Elements may represent one or more subadults.

Context	Skeletal Section	Element	Side	Estimated Age-At-Death	Source
Grave 6, Locus 1	Subadult Cranial	Mandible	N/A	10-13 years old	Baker et al. 2005; Moorrees et al. 1963

Table 7. Skeletal elements from Grave 6, Locus 1 (estimated age range: 10-13). Sides are indicated as L (left), R (right), or N/A for unsided.

Locus 2

Locus 2 is consistent with its MNI approximation of 1 as the age-at-death sample could not be estimated effectively. The limited results concluded there was a 3-5-year-old femoral neck and an ischium bone with an estimation of 1-3 years of age-at-death based on comparison to images and data collected for subadult growth (Garn et al. 1967; Baker et al. 2005; Molleson and Cox 1993). Although these estimates might appear inconsistent for one individual, the inherent error margins associated with subadult age estimations allow for some overlap. Therefore, to avoid the inflation of an MNI estimate, the elements have been grouped together to represent one individual. As a reminder, these elements represent a hypothetical individual and may originate from one or more individuals.

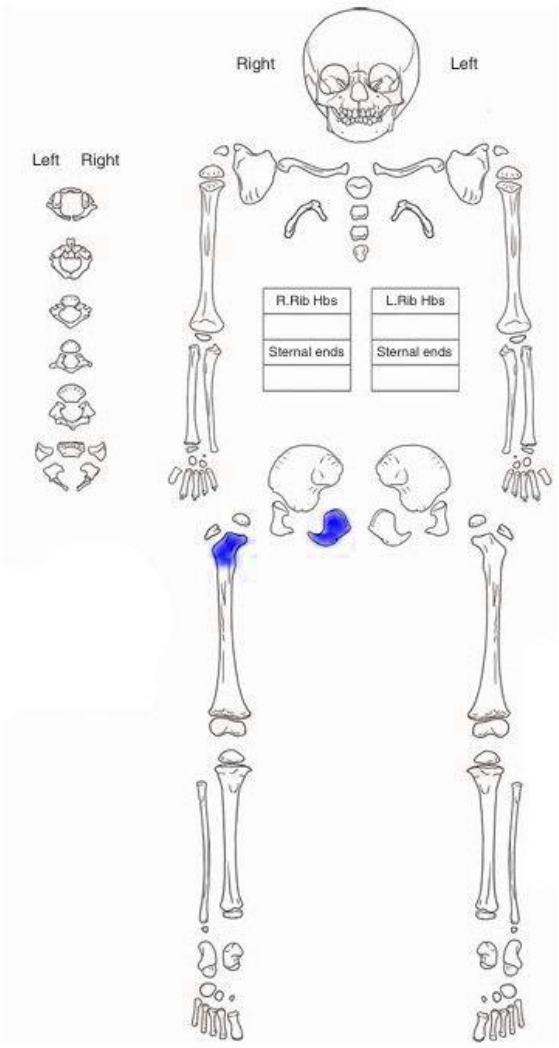


Figure 10. Skeletal elements from Grave 6, Locus 2 (estimated age range: 1-5 years), highlighted in blue. Elements may represent one or more subadults.

Context	Skeletal Section	Element	Side	Estimated Age-At-Death	Sources
Grave 6, Locus 2	Subadult Pelvic Girdle	Ischium	R	1-3 years old	Baker et al. 2005; Molleson and Cox 1993
	Subadult Lower Limb	Femur - neck	N/A	3-5 years old	Baker et al. 2005; Garn et al. 1967

Table 8. Skeletal elements from Grave 6, Locus 2 (estimated age range: 1-5 years). Sides are indicated as L (left), R (right), or N/A for unsided.

Locus 3

The Locus 3 MNI estimation was 3 individuals. All remains used to estimate age-at-death are present in Tables 9-12 below. Four distinct individuals can be estimated based on the non-overlapping elements and age estimates. The youngest elements, a proximal femur fragment and a proximal tibia fragment, were estimated as being 0 to 2 years old at the time of death. This information is illustrated in Figure 14 and Table 12. A second possible individual is estimated at approximately 5 years of age based on a proximal femoral epiphysis. This information is illustrated in Figure 13 and Table 11. A third possible individual contains a left talus with an estimated age range of 6-12 years old, and right femoral epiphysis, estimated to be 6-12 years old, represented in Figure 11 and Table 9. The oldest elements represent a possible individual from 12-18 years old, with a right proximal femur, an unsided proximal femur epiphysis, 2 right tibia fragments, and a *pars basilaris*. This is illustrated in Figure 12 and Table 10. The initial MNI estimation of 3 is not consistent with the findings of AAD. After estimating the age-at-death of each element, there are most likely minimally 4 unique individuals present.

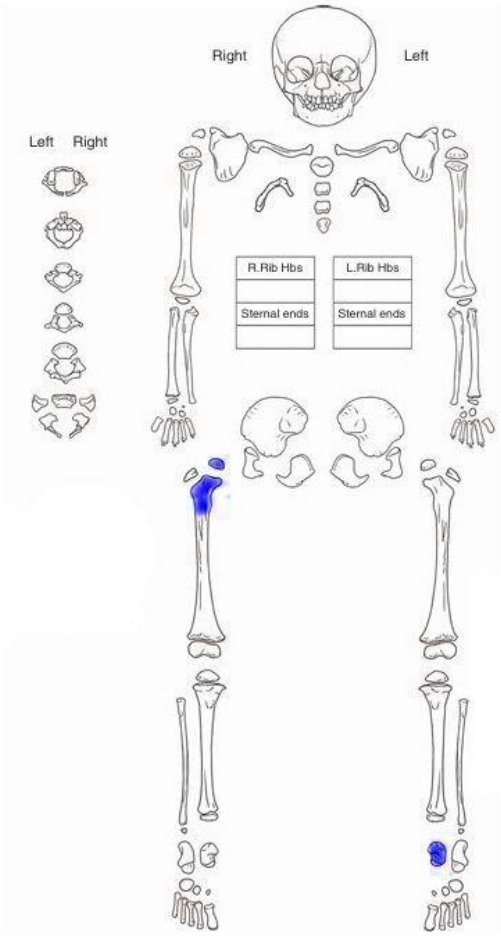


Figure 11. Skeletal elements from Grave 6, Locus 3 (estimated age range: 6-12 years), highlighted in blue. Elements may represent one or more subadults.

Context	Skeletal Section	Element	Side	Estimated Age-At-Death	Sources
Grave 6, Locus 3	Subadult Hand/Foot	Talus	L	6-12 years old	Baker et al. 2005; Cunningham et al. 2016
	Subadult Lower Limb	Femur – neck and proximal epiphyses	R	6-12 years old	Baker et al. 2005; Cardoso 2008

Table 9. Skeletal elements from Grave 6, Locus 3 (estimated age range: 6-12 years). Sides are indicated as L (left), R (right), or N/A for unsided.

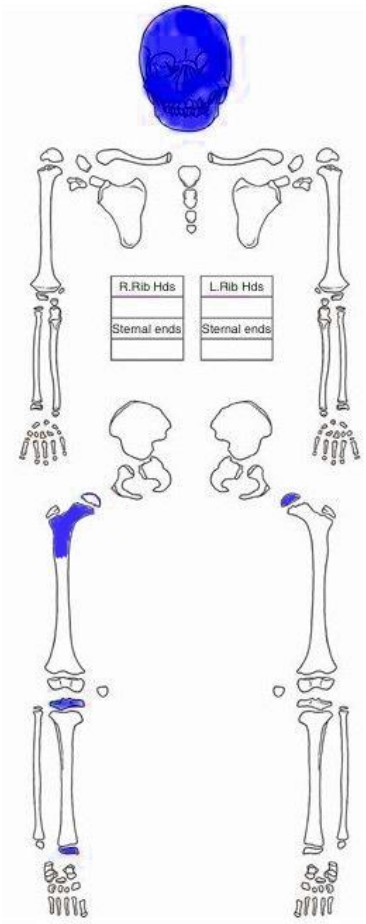


Figure 12. Skeletal elements from Grave 6, Locus 3 (estimated age range: 12-18 years), highlighted in blue. Elements may represent one or more subadults.

Context	Skeletal Section	Element	Side	Estimated Age-At-Death	Sources
Grave 6, Locus 3	Subadult Cranial	Pars Basilaris	N/A	>5 years old	Baker et al. 2005; Scheuer and MacLaughlin-Black 1994
	Subadult Lower Limb	Femur – proximal epiphysis	N/A	12-18 years old	Baker et al. 2005; Cardoso 2008; Coqueugniot and Weaver 2007; Schaefer 2008

Context	Skeletal Section	Element	Side	Estimated Age-At-Death	Sources
Grave 6, Locus 3	Subadult Lower Limb	Femur – Proximal shaft, neck, and lesser trochanter	R	14-17 years old	Baker et al. 2005; Cardoso 2008; Coqueugniot and Weaver 2007; Schaefer 2008
		Tibia – proximal epiphysis	R	12-18 years old	Baker et al. 2005; Cardoso 2008; Coqueugniot and Weaver 2007; Schaefer 2008
	Subadult Lower Limb	Tibia – distal epiphysis	R	12-18 years old	Baker et al. 2005; Cardoso 2008; Coqueugniot and Weaver 2007; Schaefer 2008

Table 10. Skeletal elements from Grave 6, Locus 3 (estimated age range: 12-18 years). Sides are indicated as L (left), R (right), or N/A for unsided.

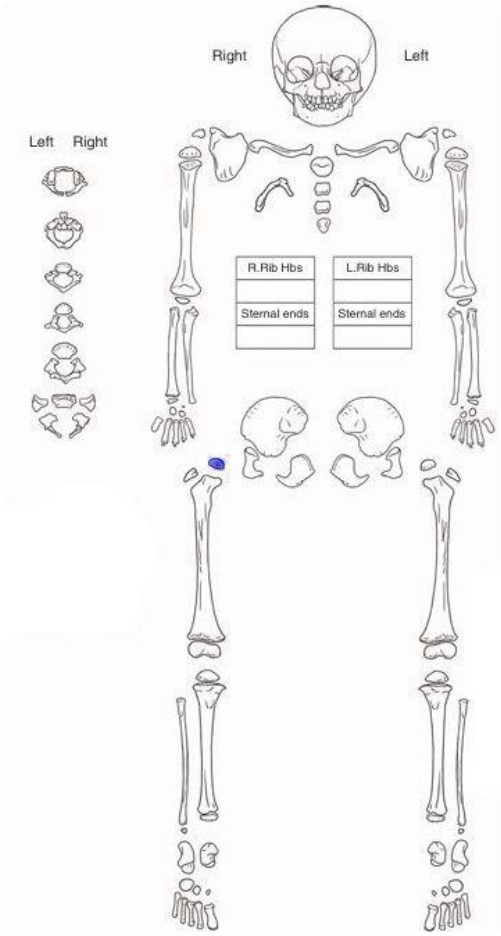


Figure 13. Skeletal elements from Grave 6, Locus 3 (estimated age range: ~5 years), highlighted in blue. Elements may represent one or more subadults.

Context	Skeletal Section	Element	Side	Estimated Age-At-Death	Sources
Grave 6, Locus 3	Subadult Lower Limb	Femur – proximal epiphysis	N/A	3- 5 years old	Baker et al. 2005; Garn et al. 1967; Schaefer et al. 2009

Table 11. Skeletal elements from Grave 6, Locus 3 (estimated age range: 3-5 years). Sides are indicated as L (left), R (right), or N/A for unsided.

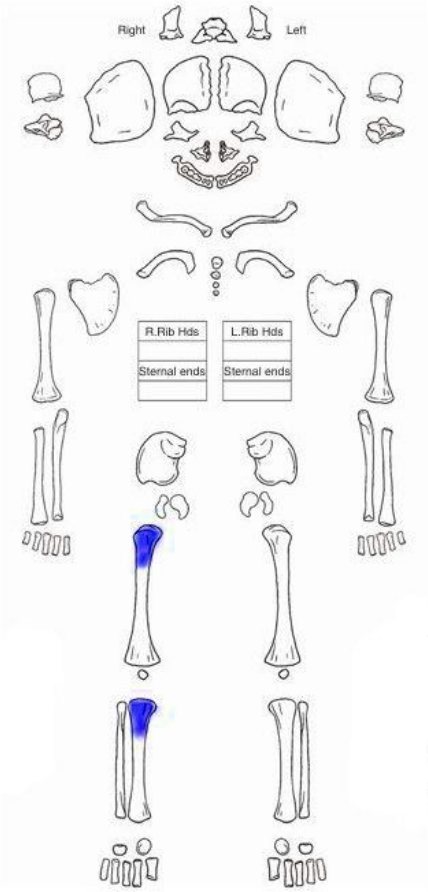


Figure 14. Skeletal elements from Grave 6, Locus 3 (estimated age range: 0-2 years), highlighted in blue. Elements may represent one or more subadults.

Context	Skeletal Section	Element	Side	Estimated Age-At-Death	Sources
Grave 6, Locus 3	Subadult Lower Limb	Femur – neck and shaft	N/A	0-1.5 years old	Baker et al. 2005; Garn et al. 1967; Schaefer et al. 2009
		Tibia – proximal end and shaft	N/A	1-2 years old	Baker et al. 2005; Schaefer et al. 2009

Table 12. Skeletal elements from Grave 6, Locus 3 (estimated age range: 0-2 years). Sides are indicated as L (left), R (right), or N/A for unsided.

Locus 4

Locus 4 does not have any reliable information for AAD, as the subadult bones found cannot be identified. An assumed MNI of 1 is given because of the presence of subadult remains, but they cannot be identified beyond this.

Locus 5

Locus 5, the largest in Grave 6, included a broad range of subadult skeletal elements spanning from fetal developmental stages to adolescent. Given the volume of associated skeletal elements, a full inventory of interpreted individuals will not be represented in text, but is available in the accompanying figures and tables. The youngest skeletal element identified was a fibula shaft, likely from the 3rd trimester of pregnancy. The oldest skeletal element identified was a right clavicle with an estimated age of 14-23 years old. The initial Locus 5 MNI estimation produced 7 individuals, however, age-at-death estimations in combination with non-overlapping skeletal elements suggest at least 14 possible individuals could be present within Locus 5. Figures 15-28 and Tables 13-26 illustrate skeletal elements grouped together for their estimated age-at-death. These groupings are interpretive and intended to showcase how a minimum count for the MNI was achieved when considering age-at-death estimations. Some groupings share overlapping age ranges—for example, multiple figures contain elements estimated between 10–22 years—these were treated as potentially representing separate individuals when anatomical duplication occurred. For instance, Figure 15 includes a left proximal humerus, a right distal ulnar epiphysis, a right and left lunate, two calcaneus fragments, a right and left femur, a left tibial epiphysis, and a right fibular epiphysis. Figure 16 contains one lunate, one right and one unsided calcaneus, a right femoral greater trochanter, distal epiphysis, and proximal neck and shaft, as well as a left femoral distal epiphysis and a left tibial distal epiphysis. The overlapping

elements from skeletal regions across both figures made it anatomically impossible to collapse these profiles into a single individual, even if their estimated age-at-death ranges overlapped. In some instances, grouping produced wider age ranges due to the developmental span of the included elements, but anatomical consistency was always maintained to avoid over- or underestimation.

Overall, within this locus 7 individuals were estimated using MNI, while the age-at-death estimations helped refine overlapping elements and distinct age ranges, supporting a higher estimation of individuals is possible.

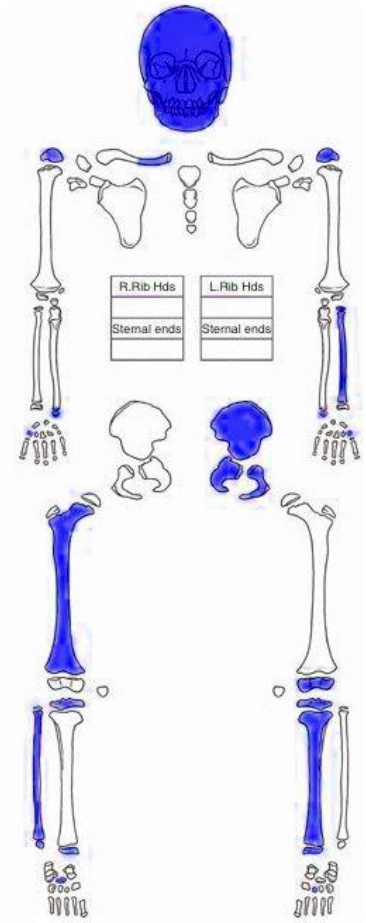


Figure 15. Skeletal elements from Grave 6, Locus 5 (estimated age range: 10-20 years), highlighted in blue. Elements may represent one or more subadults.

Context	Skeletal Section	Element	Side	Estimated Age-At-Death	Sources
Grave 6, Locus 5	Subadult Cranial	Pars Basilaris	N/A	>5 years old	Baker et al. 2005; Scheuer and MacLaughlin-Black 1994
	Subadult Upper Limb	Humerus – proximal epiphysis	R	12-18 years old	Baker et al. 2005; Coqueugniot and Weaver 2007; Schaefer 2008; Schaefer et al. 2009
		Humerus – proximal epiphysis	N/A	12-18 years old	Baker et al. 2005; Coqueugniot and Weaver 2007; Schaefer 2008; Schaefer et al. 2009
		Ulna – distal epiphysis	L	14-20 years old	Baker et al. 2005; Coqueugniot and Weaver 2007; Schaefer 2008; Schaefer et al. 2009
		Ulna – distal epiphysis	R	12-18 years old	Baker et al. 2005; Coqueugniot and Weaver 2007; Schaefer 2008; Schaefer et al. 2009

Context	Skeletal Section	Element	Side	Estimated Age-At-Death	Sources
Grave 6, Locus 5	Subadult Upper Limb	Radius – proximal epiphysis	N/A	12-18 years old	Baker et al. 2005; Coqueugniot and Weaver 2007; Schaefer 2008; Schaefer et al. 2009
	Subadult Pectoral Girdle	Clavicle – sternal end	R	14-23 years old	Baker et al. 2005; Schaefer 2008; Schaefer et al. 2009; Rissecch and Black 2007; Webb and Suchey 1985
	Subadult Hand/Foot	Lunate	L	15-20 years old	Baker et al. 2005; Schaefer et al. 2009
	Subadult Hand/Foot	Lunate	R	15-20 years old	Baker et al. 2005; Schaefer et al. 2009
		Cuneiform	L	15-20 years old	Baker et al. 2005; Schaefer et al. 2009
		Calcaneus – epiphysis	N/A	10-20 years old	Baker et al. 2005; Schaefer et al. 2009
		Calcaneus – epiphysis	N/A	10-20 years old	Baker et al. 2005; Schaefer et al. 2009
	Subadult pelvic girdle	Os coxa	L	17-22 years old	Baker et al. 2005; Schaefer 2008
	Subadult Lower Limb	Femur	R	12-18 years old	Baker et al. 2005; Cardoso 2008; Coqueugniot and Weaver 2007; Schaefer 2008

Context	Skeletal Section	Element	Side	Estimated Age-At-Death	Sources
Grave 6, Locus 5	Subadult Lower Limb	Femur – distal epiphysis	L	12-18 years old	Baker et al. 2005; Cardoso 2008; Coqueugniot and Weaver 2007; Schaefer 2008
		Tibia – proximal epiphysis	R	12-18 years old	Baker et al. 2005; Cardoso 2008; Coqueugniot and Weaver 2007; Schaefer 2008
		Tibia – proximal shaft end and shaft	N/A	12-18 years old	Baker et al. 2005; Cardoso 2008; Coqueugniot and Weaver 2007; Schaefer 2008
		Tibia – distal epiphysis	L	14-18 years old	Baker et al. 2005; Cardoso 2008; Coqueugniot and Weaver 2007; Schaefer 2008
		Tibia – distal epiphysis	R	13-18 years old	Baker et al. 2005; Cardoso 2008; Coqueugniot and Weaver 2007; Schaefer 2008
		Fibula	R	12-18 years old	Baker et al. 2005; Cardoso 2008; Coqueugniot and Weaver 2007;

Table 13. Skeletal elements from Grave 6, Locus 5 (estimated age range: 10-20 years). Sides are indicated as L (left), R (right), or N/A for unsided.

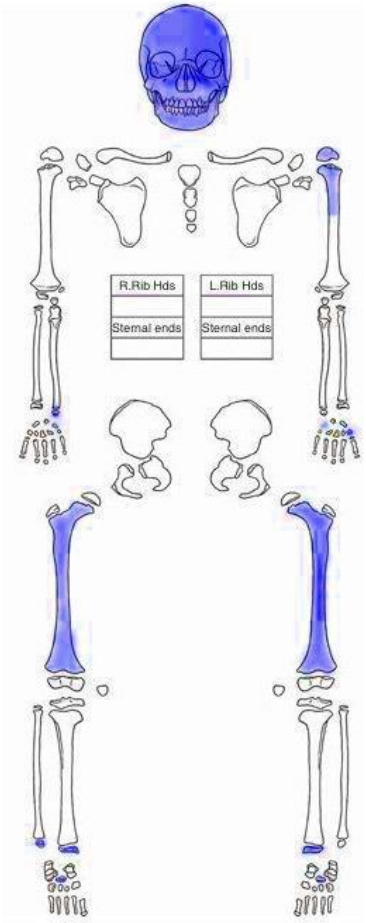


Figure 16. Skeletal elements from Grave 6, Locus 5 (estimated age range: 10-20 years), highlighted in blue. Elements may represent one or more subadults.

Context	Skeletal Section	Element	Side	Estimated Age-At-Death	Sources
Grave 6, Locus 5	Subadult Cranial	Pars Basilaris	N/A	>5 years old	Baker et al. 2005; Scheuer and MacLaughlin-Black 1994
	Subadult Upper Limb	Humerus – proximal epiphysis and shaft	L	12-18 years old	Baker et al. 2005; Coqueugniot and Weaver 2007; Schaefer 2008; Schaefer et al. 2009
		Ulna – distal epiphysis	R	12-18 years old	Baker et al. 2005; Coqueugniot and Weaver 2007; Schaefer 2008; Schaefer et al. 2009
	Subadult Hand/Foot	Lunate	R	15-20 years old	Baker et al. 2005; Schaefer et al. 2009
		Lunate	L	15-20 years old	Baker et al. 2005; Schaefer et al. 2009
		Calcaneus – epiphysis	N/A	10-20 years old	Baker et al. 2005; Schaefer et al. 2009
		Calcaneus – epiphysis	N/A	10-20 years old	Baker et al. 2005; Schaefer et al. 2009
	Subadult Lower Limb	Femur	L	12-16 years old	Baker et al. 2005; Cardoso 2008; Coqueugniot and Weaver 2007; Schaefer 2008

Context	Skeletal Section	Element	Side	Estimated Age-At-Death	Sources
Grave 6, Locus 5	Subadult Lower Limb	Femur	R	14-19 years old	Baker et al. 2005; Cardoso 2008; Coqueugniot and Weaver 2007; Schaefer 2008
Grave 6, Locus 5	Subadult Lower Limb	Tibia – distal epiphysis	L	12-18 years old	Baker et al. 2005; Cardoso 2008; Coqueugniot and Weaver 2007; Schaefer 2008
		Fibula – epiphysis	R	12-16 years old	Baker et al. 2005; Cardoso 2008; Coqueugniot and Weaver 2007;

Table 14. Skeletal elements from Grave 6, Locus 5 (estimated age range: 10-20 years). Sides are indicated as L (left), R (right), or N/A for unsided.

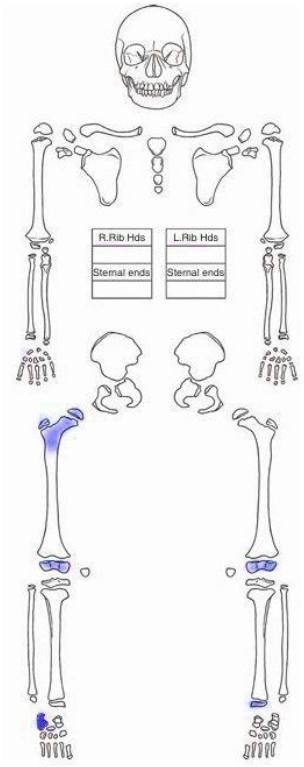


Figure 17. Skeletal elements from Grave 6, Locus 5 (estimated age range: 10-20 years), highlighted in blue. Elements may represent one or more subadults.

Context	Skeletal Section	Element	Side	Estimated Age-At-Death	Sources
Grave 6, Locus 5	Subadult Hand/Foot	Lunate	N/A	15-20 years old	Baker et al. 2005; Schaefer et al. 2009
		Calcaneus	R	12-15 years old	Baker et al. 2005; Schaefer et al. 2009
		Calcaneus – epiphysis	N/A	10-20 years old	Baker et al. 2005; Schaefer et al. 2009
	Subadult Lower Limb	Femur – greater trochanter	R	12-15 years old	Baker et al. 2005; Cardoso 2008; Coqueugniot and Weaver 2007; Schaefer 2008

Context	Skeletal Section	Element	Side	Estimated Age-At-Death	Sources
Grave 6, Locus 5	Subadult Lower Limb	Femur – distal epiphysis	R	12-18 years old	Baker et al. 2005; Cardoso 2008; Coqueugniot and Weaver 2007; Schaefer 2008
		Femur – proximal shaft and neck	R	12-18 years old	Baker et al. 2005; Cardoso 2008; Coqueugniot and Weaver 2007; Schaefer 2008
		Femur – distal epiphysis	L	14-19 years old	Baker et al. 2005; Cardoso 2008; Coqueugniot and Weaver 2007; Schaefer 2008
		Tibia – distal epiphysis	L	12-18 years old	Baker et al. 2005; Cardoso 2008; Coqueugniot and Weaver 2007; Schaefer 2008

Table 15. Skeletal elements from Grave 6, Locus 5 (estimated age range: 10-20 years). Sides are indicated as L (left), R (right), or N/A for unsided.

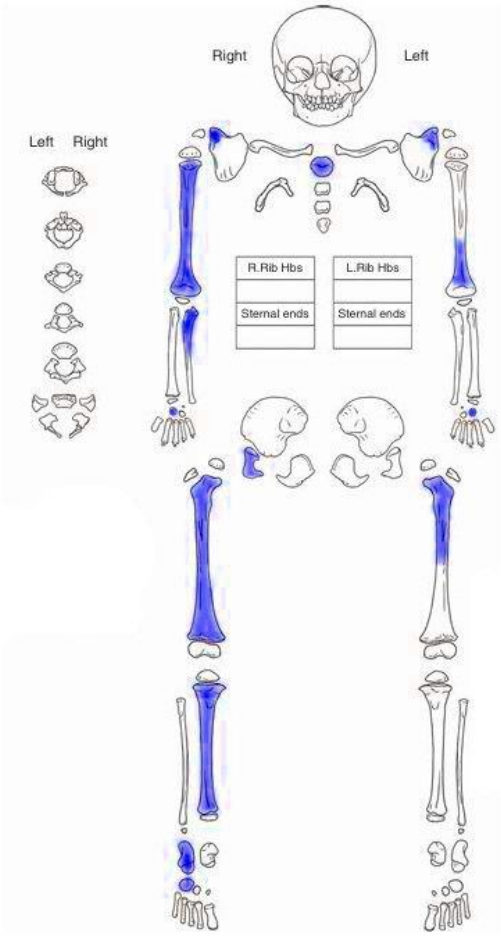


Figure 18. Skeletal elements from Grave 6, Locus 5 (estimated age range: 3-9 years), highlighted in blue. Elements may represent one or more subadults.

Context	Skeletal Section	Element	Side	Estimated Age-At-Death	Sources
Grave 6, Locus 5	Subadult Upper Limb	Humerus	R	5-7 years old	Baker et al. 2005; Garn et al. 1967; Ogden et al. 1978;
		Humerus – distal shaft	N/A	>5 years old	Baker et al. 2005; Garn et al. 1967; Ogden et al. 1978;
	Subadult Upper Limb	Ulna – proximal shaft end	R	5-8 years old	Baker et al. 2005; Garn et al. 1967; Schaefer et al. 2009

Context	Skeletal Section	Element	Side	Estimated Age-At-Death	Sources
Grave 6, Locus 5	Subadult Pectoral Girdle	Scapula – glenoid fossa	R	7-8 years old	Baker et al. 2005; Saunders 2008
		Scapula – glenoid fossa	N/A	7-8 years old	Baker et al. 2005; Saunders 2008
		Manubrium	N/A	3-8 years old	Baker et al. 2005; Jit and Kaur 1989
	Subadult Hand/Foot	Cuboid	R	5-8 years old	Baker et al. 2005; Schaefer et al. 2009
		Lunate	L	5-8 years old	Baker et al. 2005; Schaefer et al. 2009
		Lunate	R	5-8 years old	Baker et al. 2005; Schaefer et al. 2009
		Calcaneus	R	5-8 years old	Baker et al. 2005; Schaefer et al. 2009
	Subadult Pelvic Girdle	Pubis	N/A	<8 years old	Baker et al. 2005; Schaefer et al. 2009
	Subadult Lower Limb	Femur	R	3-5 years old	Baker et al. 2005; Garn et al. 1967
		Femur – neck and shaft	L	3-5 years old	Baker et al. 2005; Garn et al. 1967
		Tibia	R	6-9 years old	Baker et al. 2005; Schaefer et al. 2009

Table 16. Skeletal elements from Grave 6, Locus 5 (estimated age range: 3-9 years). Sides are indicated as L (left), R (right), or N/A for unsided.

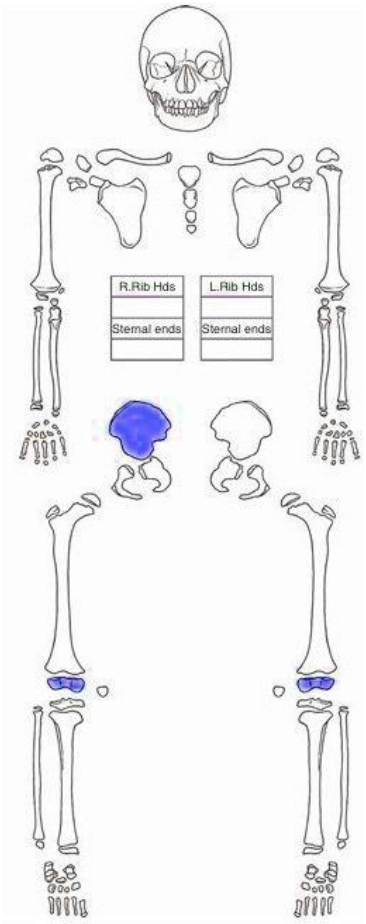


Figure 19. Skeletal elements from Grave 6, Locus 5 (estimated age range: 9-20 years), highlighted in blue. Elements may represent one or more subadults.

Context	Skeletal Section	Element	Side	Estimated Age-At-Death	Sources
Grave 6, Locus 5	Subadult Pelvic Girdle	Ilium	N/A	9-20 years old	Coqueugniot and Weaver 2007; Schaefer et al. 2009
	Subadult Lower Limb	Femur- distal epiphysis	N/A	12-18 years old	Baker et al. 2005; Cardoso 2008; Coqueugniot and Weaver 2007; Schaefer 2008

Context	Skeletal Section	Element	Side	Estimated Age-At-Death	Sources
		Femur – distal epiphysis	R	12-18 years old	Baker et al. 2005; Cardoso 2008; Coqueugniot and Weaver 2007; Schaefer 2008

Table 17. Skeletal elements from Grave 6, Locus 5 (estimated age range: 9-20 years). Sides are indicated as L (left), R (right), or N/A for unsided.

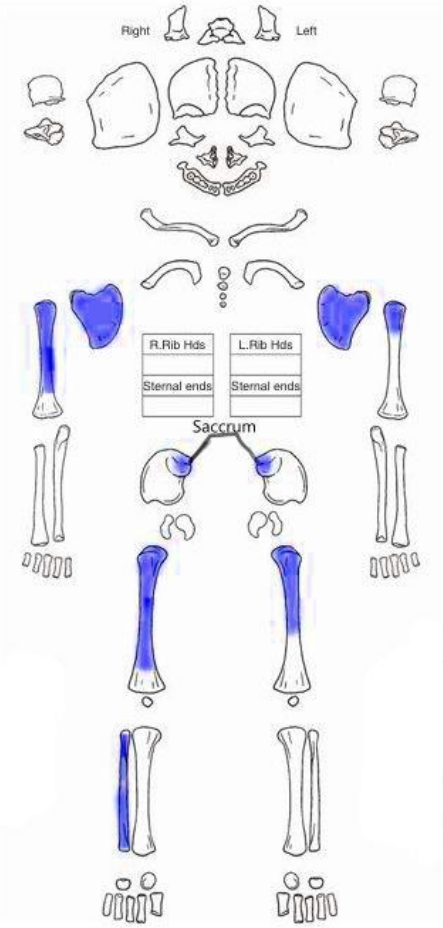


Figure 20. Skeletal elements from Grave 6, Locus 5 (estimated age range: 40 weeks - 3 years), highlighted in blue. Elements may represent one or more subadults.

Context	Skeletal Section	Element	Side	Estimated Age-At-Death	Sources
Grave 6, Locus 5	Subadult Upper Limb	Humerus – proximal epiphysis	N/A	1-2 years old	Baker et al. 2005; Schaefer et al. 2009
		Humerus – proximal shaft	R	1-5 years old	Baker et al. 2005; Schaefer
Grave 6, Locus 5	Subadult Pectoral Girdle	Scapula	N/A	0–1-year-old	Baker et al. 2005; Fazekas and Kosa 1978
		Scapula	N/A	0–1-year-old	Baker et al. 2005; Fazekas and Kosa 1978
	Subadult Pelvic Girdle	Sacrum	N/A	0–1-year-old	Baker et al. 2005; Schaefer et al. 2009
	Subadult Lower Limb	Femur – neck and proximal shaft	L	1-2 years old	Baker et al. 2005; Garn et al. 1967
		Femur – shaft	N/A	1.5 years old	Baker et al. 2005; Garn et al. 1967
	Subadult Lower Limb	Fibula – shaft	N/A	40 weeks -1-year-old	Baker et al. 2005; Fazekas and Kosa 1978
		Femur – neck and proximal shaft	R	1-3 years old	Baker et al. 2005; Garn et al. 1967

Table 18. Skeletal elements from Grave 6, Locus 5 (estimated age range: 40 weeks - 3 years). Sides are indicated as L (left), R (right), or N/A for unsided.

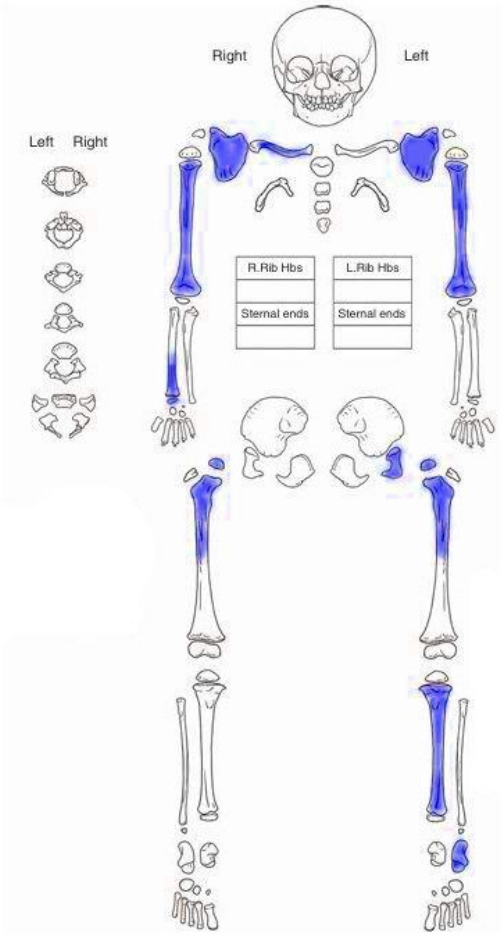


Figure 21. Skeletal elements from Grave 6, Locus 5 (estimated age range: 2-8 years), highlighted in blue. Elements may represent one or more subadults.

Context	Skeletal Section	Element	Side	Estimated Age-At-Death	Sources
Grave 6, Locus 5	Subadult Upper Limb	Humerus	N/A	3-8 years old	Baker et al. 2005; Schaefer et al. 2009
		Humerus	N/A	3-5 years old	Baker et al. 2005; Schaefer et al. 2009
		Radius – distal shaft and epiphysis	N/A	3-5 years old	Baker et al. 2005; Schaefer et al. 2009
	Subadult Pectoral Girdle	Scapula	R	5-6 years old	Baker et al. 2005; Schaefer et al. 2009

Context	Skeletal Section	Element	Side	Estimated Age-At-Death	Sources
Grave 6, Locus 5	Subadult Pectoral Girdle	Scapula	N/A	3-6 years old	Baker et al. 2005; Schaefer et al. 2009
	Subadult Hand/Foot	Calcaneus	L	2-3 years old	Baker et al. 2005; Schaefer et al. 2009
	Subadult Pelvic Girdle	Pubis	L	2-6 years old	Baker et al. 2005; Schaefer et al. 2009
	Subadult Lower Limb	Femur – proximal shaft and neck	R	3-5 years old	Baker et al. 2005; Garn et al. 1967; Schaefer et al. 2009
		Femur – proximal shaft	L	3-5 years old	Baker et al. 2005; Garn et al. 1967; Schaefer et al. 2009
		Tibia	L	3-5 years old	Baker et al. 2005; Schaefer et al. 2009

Table 19. Skeletal elements from Grave 6, Locus 5 (estimated age range: 2-8 years). Sides are indicated as L (left), R (right), or N/A for unsided.

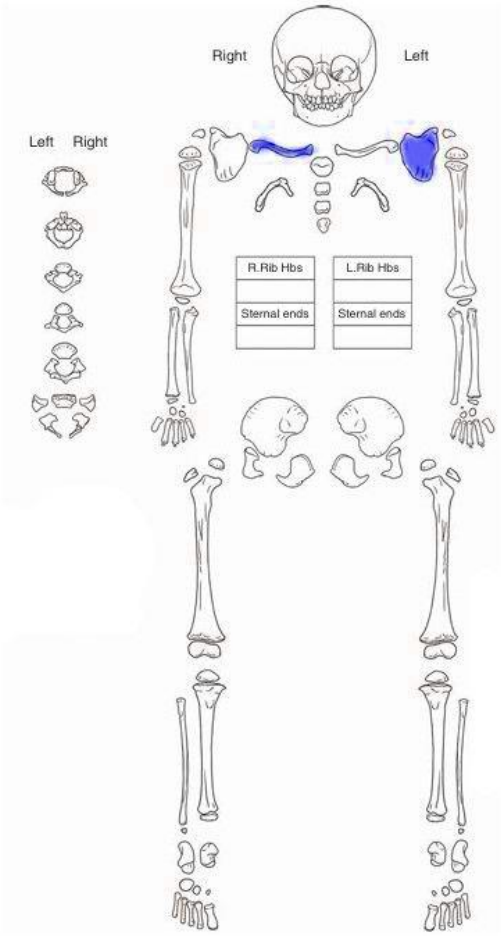


Figure 22. Skeletal elements from Grave 6, Locus 5 (estimated age range: 2-6 years), highlighted in blue. Elements may represent one or more subadults.

Context	Skeletal Section	Element	Side	Estimated Age-At-Death	Sources
Grave 6, Locus 5	Subadult Pectoral Girdle	Scapula	L	5-6 years old	Baker et al. 2005; Rissech and Black 2007; Schaefer et al. 2009
		Clavicle – shaft and epiphysis	R	2-5 years old	Baker et al. 2005; Schaefer et al. 2009

Table 20. Skeletal elements from Grave 6, Locus 5 (estimated age range: 2-6 years). Sides are indicated as L (left), R (right), or N/A for unsided.

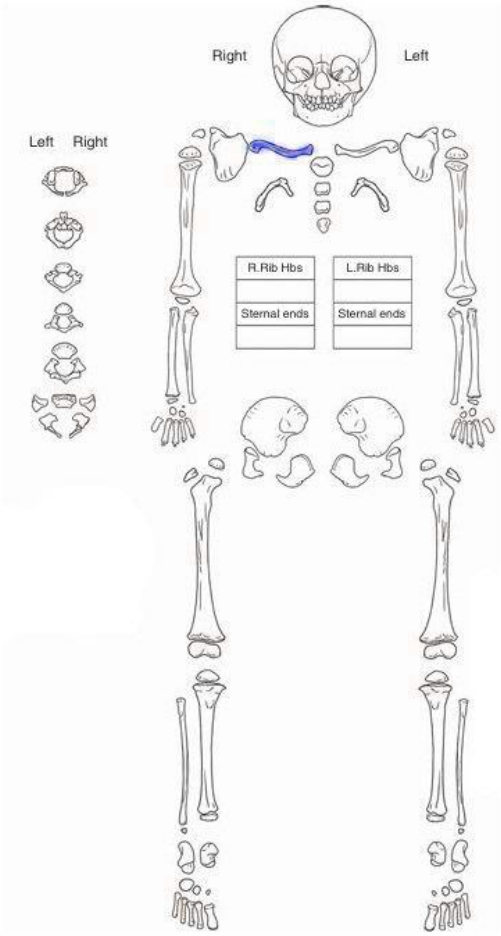


Figure 23. Skeletal elements from Grave 6, Locus 5 (estimated age range: 2-5 years), highlighted in blue. Elements may represent one or more subadults.

Context	Skeletal Section	Element	Side	Estimated Age-At-Death	Sources
Grave 6, Locus 5	Subadult Pectoral Girdle	Clavicle – shaft and epiphysis	R	2-5 years old	Baker et al. 2005; Schaefer et al. 2009

Table 21. Skeletal elements from Grave 6, Locus 5 (estimated age range: 2-5 years). Sides are indicated as L (left), R (right), or N/A for unsided.

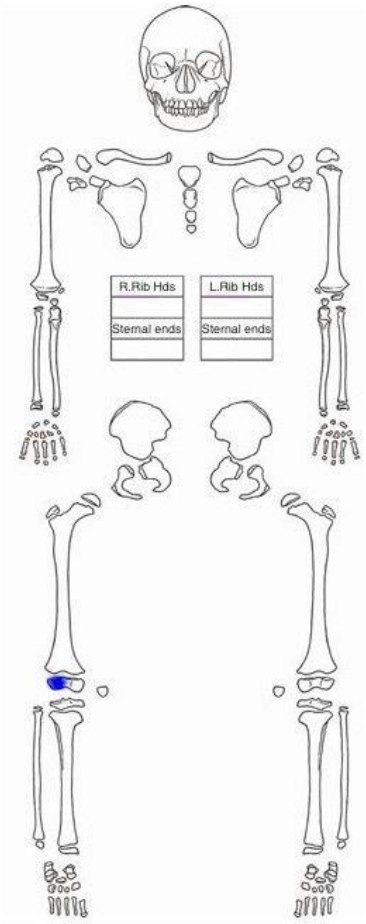


Figure 24. Skeletal elements from Grave 6, Locus 5 (estimated age range: 12-18 years), highlighted in blue. Elements may represent one or more subadults.

Context	Skeletal Section	Element	Side	Estimated Age-At-Death	Sources
Grave 6, Locus 5	Subadult Lower Limb	Femur – lateral half of distal epiphysis	N/A	12-18 years old	Baker et al. 2005; Cardoso 2008; Coqueugniot and Weaver 2007; Schaefer 2008

Table 22. Skeletal elements from Grave 6, Locus 5 (estimated age range: 12-18 years). Sides are indicated as L (left), R (right), or N/A for unsided.

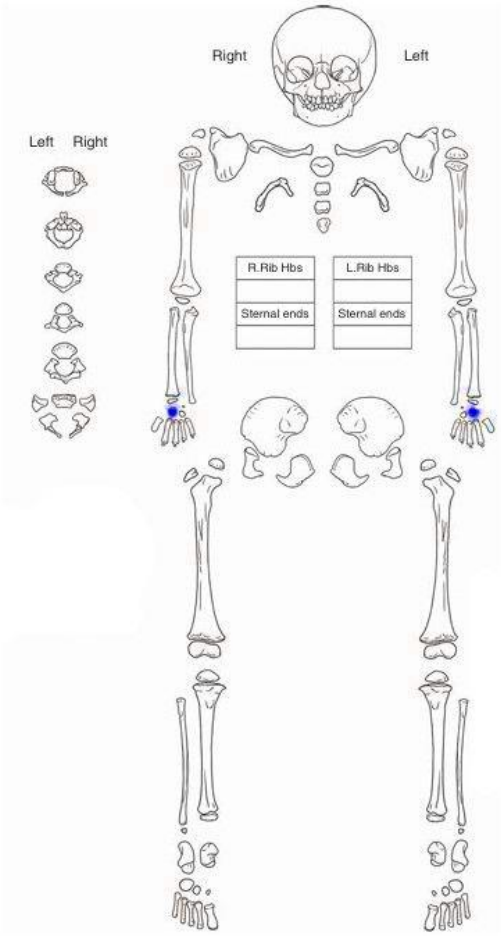


Figure 25. Skeletal elements from Grave 6, Locus 5 (estimated age range: ~8 years), highlighted in blue. Elements may represent one or more subadults.

Context	Skeletal Section	Element	Side	Estimated Age-At-Death	Sources
Grave 6, Locus 5	Subadult Hand/Foot	Lunate	N/A	7-8 years old	Baker et al. 2005; Schaefer et al. 2009
		Lunate	N/A	7-8 years old	Baker et al. 2005; Schaefer et al. 2009

Table 23. Skeletal elements from Grave 6, Locus 5 (estimated age range: ~8 years). Sides are indicated as L (left), R (right), or N/A for unsided.

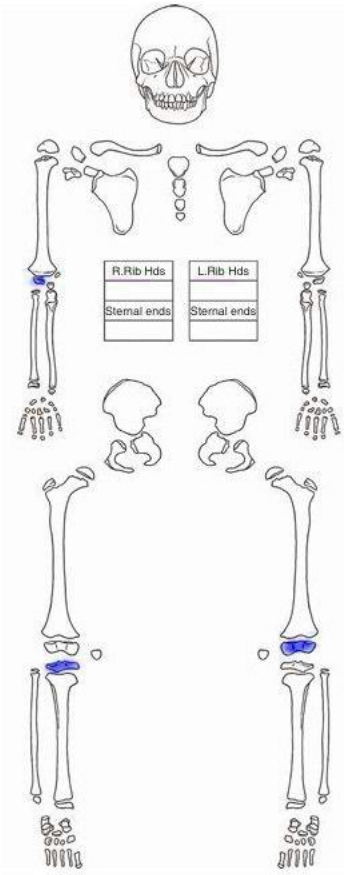


Figure 26. Skeletal elements from Grave 6, Locus 5 (estimated age range: 5-14 years), highlighted in blue. Elements may represent one or more subadults.

Context	Skeletal Section	Element	Side	Estimated Age-At-Death	Sources
Grave 6, Locus 5	Subadult Upper limb	Humerus – distal epiphysis	R	>5 years old	Baker et al. 2005; Schaefer et al. 2009
	Subadult Lower Limb	Femur – distal epiphysis	L	10-12 years old	Baker et al. 2005; Garn et al. 1967; Schaefer et al. 2009
		Tibia – proximal epiphysis	N/A	5-14 years old	Baker et al. 2005; Garn et al. 1967; Schaefer et al. 2009

Table 24. Skeletal elements from Grave 6, Locus 5 (estimated age range: 5-14 years). Sides are indicated as L (left), R (right), or N/A for unsided.

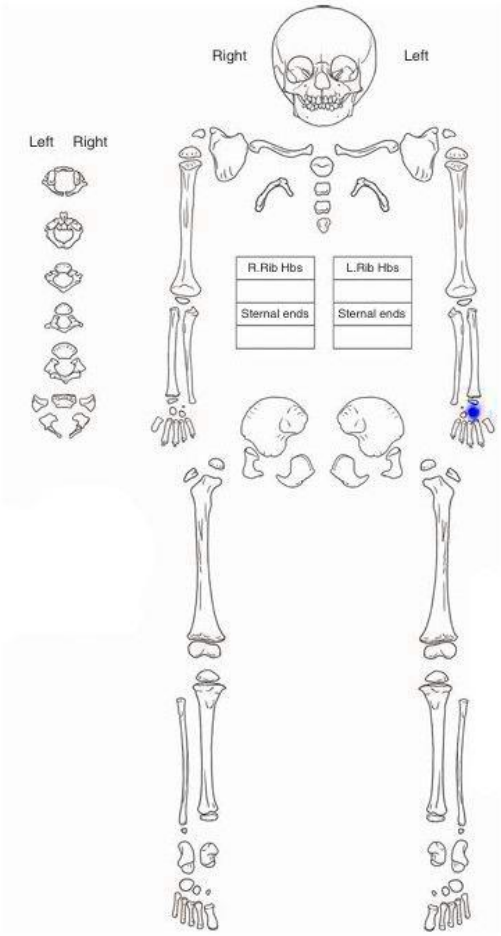


Figure 27. Skeletal elements from Grave 6, Locus 5 (estimated age range: ~8 years), highlighted in blue. Elements may represent one or more subadults.

Context	Skeletal Section	Element	Side	Estimated Age-At-Death	Sources
Grave 6, Locus 5	Subadult Hand/Foot	Lunate	L	7-8 years old	Baker et al. 2005; Schaefer et al. 2009

Table 25. Skeletal elements from Grave 6, Locus 5 (estimated age range: ~8 years). Sides are indicated as L (left), R (right), or N/A for unsided.

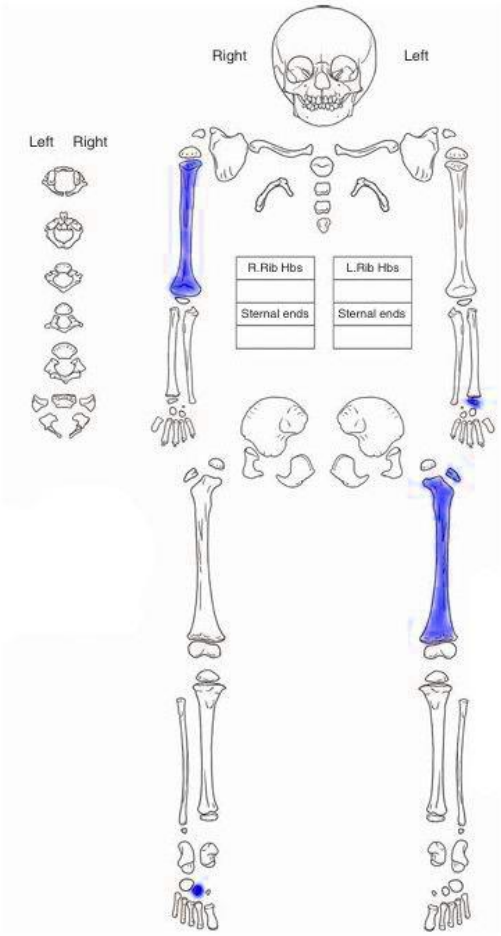


Figure 28. Skeletal elements from Grave 6, Locus 5 (estimated age range: 5-12 years), highlighted in blue. Elements may represent one or more subadults.

Context	Skeletal Section	Element	Side	Estimated Age-At-Death	Sources
Grave 6, Locus 5	Subadult Upper Limb	Humerus	R	5-12 years old	Baker et al. 2005; Garn et al. 1967; Schaefer et al. 2009
		Radius – distal epiphysis	L	9-12 years old	Baker et al. 2005; Garn et al. 1967; Schaefer et al. 2009
	Subadult Hand/Foot	2nd Cuneiform	N/A	9-12 years old	Baker et al. 2005; Schaefer et al. 2009

Context	Skeletal Section	Element	Side	Estimated Age-At-Death	Sources
	Subadult Lower Limb	Femur	L	6-12 years old	Baker et al. 2005; Garn et al. 1967; Schaefer et al. 2009
		Femur – greater trochanter	N/A	6-12 years old	Baker et al. 2005; Garn et al. 1967; Schaefer et al. 2009

Table 26. Skeletal elements from Grave 6, Locus 5 (estimated age range: 5-12 years). Sides are indicated as L (left), R (right), or N/A for unsided.

Locus 6

The lowest level of Grave 6, Locus 6, bore subadult remains with age-at-death estimates falling between 0 and 5 years of age. There are 10 elements between ages 0-5 years old. This locus MNI estimate was 3, as the AAD results would suggest this is accurate**.**

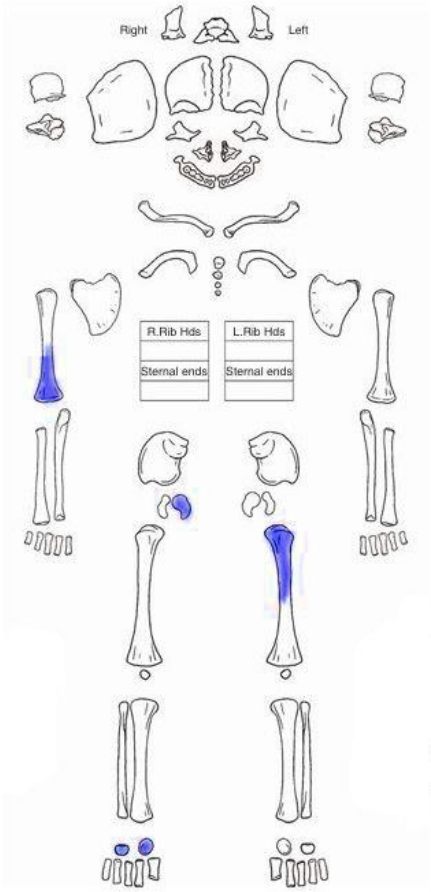


Figure 29. Skeletal elements from Grave 6, Locus 5 (estimated age range: 0-3 years), highlighted in blue. Elements may represent one or more subadults.

Context	Skeletal Section	Element	Side	Estimated Age-At-Death	Sources
Grave 6, Locus 6	Subadult Upper Limb	Humerus – distal shaft	R	0–1-year-old	Baker et al. 2005; Garn et al. 1967; Schaefer et al. 2009
	Subadult Hand/Foot	Talus	R	2-3 years old	Baker et al. 2005; Schaefer et al. 2009
		Calcaneus	R	2-3 years old	Baker et al. 2005; Schaefer et al. 2009

Context	Skeletal Section	Element	Side	Estimated Age-At-Death	Sources
Grave 6, Locus 6	Subadult Pelvic Girdle	Ischium	N/A	0–1-year-old	Baker et al. 2005; Schaefer et al. 2009
	Subadult Lower Limb	Femur – proximal shaft and neck	L	1-2 years old	Baker et al. 2005; Garn et al. 1967; Schaefer et al. 2009

Table 27. Skeletal elements from Grave 6, Locus 5 (estimated age range: 0-3 years). Sides are indicated as L (left), R (right), or N/A for unsided.

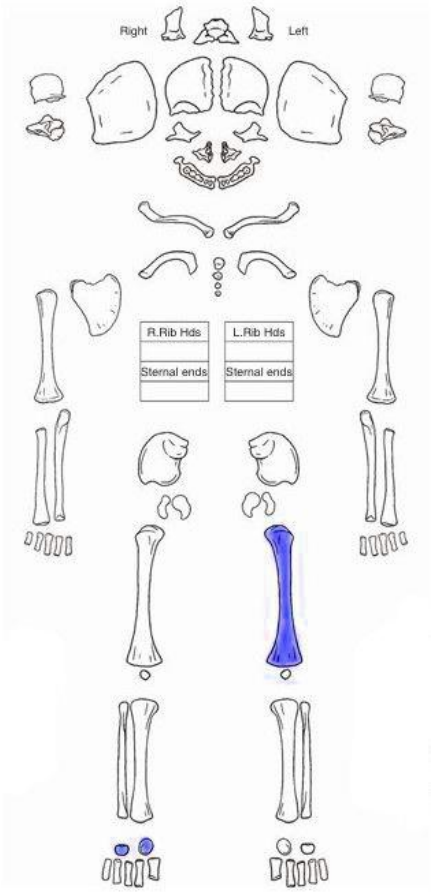


Figure 30. Skeletal elements from Grave 6, Locus 5 (estimated age range: 1.5-3 years), highlighted in blue. Elements may represent one or more subadults.

Context	Skeletal Section	Element	Side	Estimated Age-At-Death	Sources
Grave 6, Locus 6	Subadult Hand/Foot	Talus	R	2-3 years old	Baker et al. 2005; Schaefer et al. 2009
		Calcaneus	R	2-3 years old	Baker et al. 2005; Schaefer et al. 2009
	Subadult Lower Limb	Femur – shaft	L	1-2 years old	Baker et al. 2005; Garn et al. 1967; Schaefer et al. 2009

Table 28. Skeletal elements from Grave 6, Locus 5 (estimated age range: 1.5-3 years). Sides are indicated as L (left), R (right), or N/A for unsided.

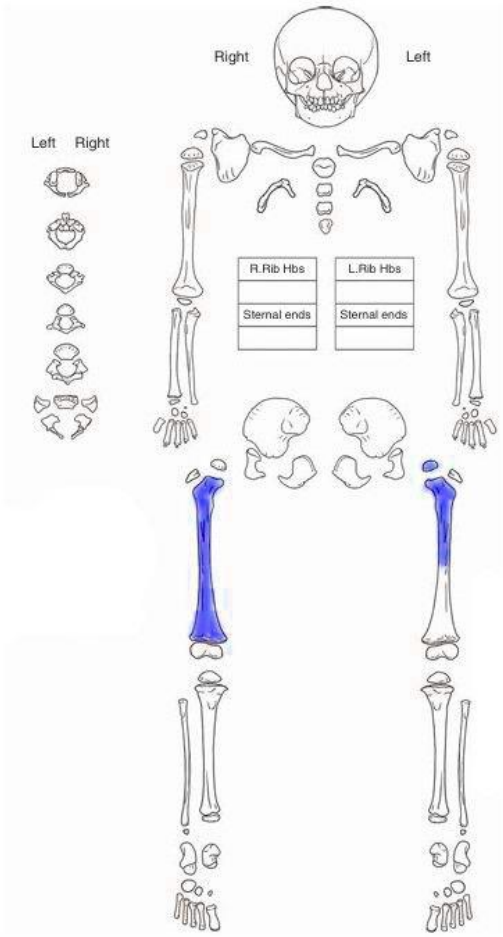


Figure 31. Skeletal elements from Grave 6, Locus 5 (estimated age range: ~5 years), highlighted in blue. Elements may represent one or more subadults.

Context	Skeletal Section	Element	Side	Estimated Age-At-Death	Sources
Grave 6, Locus 6	Subadult Lower Limb	Femur	R	3-5 years old	Baker et al. 2005; Garn et al. 1967; Schaefer et al. 2009
		Femur – proximal shaft and neck	N/A	3-5 years old	Baker et al. 2005; Garn et al. 1967; Schaefer et al. 2009

Table 29. Skeletal elements from Grave 6, Locus 5 (estimated age range: ~5 years). Sides are indicated as L (left), R (right), or N/A for unsided.

Chapter 6 – Discussion

6.1 *Minimum Number of Individuals (MNI)*

The use of the Landmark System to estimate the MNI of Grave 6 was a straightforward process. Within the six loci, a minimum of 17 subadult individuals were identified. The modified subadult Landmark System presented in this thesis provided a systematic way to separate individuals with little overlap or cause for confusion on small skeletal elements. More specifically, the modified method helped clarify the large number of repeating elements found in Locus 5. Using the help of colour coordination and the drawn landmark images for subadult bones, remains from Locus 5 was able to be examined consistently and rapidly. This demonstrates that the modifications made and the images drawn are useful when working with commingled and fragmentary subadult skeletal assemblages. Modified subadult landmark images were supplemented with examination of real subadult bone and standard subadult bone casts (Bone Clones) (available in the bioanthropology lab at UWaterloo). These collections were used in tandem with the images drawn to provide the highest confidence estimate of landmarks. Using the 3D collections and the images, the Landmark System provide a significant tool for combating common challenges faced with commingled and fragmentary subadult assemblages such as preservation and completeness of bones.

It is important to keep in mind that this is a minimum estimate, making it likely that 17 is a low number and not the actual number of individuals who were interred in Grave 6. Nine hundred and eighty-four subadult bones were collected across all 6 loci, with 439 being suitable for analysis, approximately 45% of the found assemblage. However, it was better than using the traditional method of MNI from White (1953), as this has resulted in low figures considering the how rare it was to find a complete bone within each locus at WF100 within Grave 6. An analysis

of viable elements was performed using the traditional MNI method for comparison, and found there to 4 elements complete enough to consider; 1 right humerus, 1 right femur, 1 left femur, and 1 mandible. As all 4 elements could be from one individual, the MNI using the traditional method would be 1.

6.1.1 *Limitations for estimating MNI*

Due to the nature of this study, there are several limitations that should be addressed. Grave 6 is a new collection, with myself being the first person to determine the subadult MNI. Because of this, there is no MNI estimation that can guarantee how successful this method was. It can be seen that the number of elements used was greater than using the traditional MNI method, however, it cannot be determined if the suggested MNI is correct.

One important factor that likely influenced the ease and outcome of this method was the condition of the remains. Grave 6 had some minimal looting activity (relative to other charnel houses at WF100) with remains from Loci 2 through 6 being undisturbed (Adams et al. 2023). Animal and insect activity was found throughout the grave loci when sorting the remains before initial assessment was performed. Some small cylindrical compacted dirt tubes were found while handling subadult remains, having come loose during examination. This greatly comprised the bone structure, subsequently breaking the subadult bone in the process in some cases. Preservation likely played a role in the clarity of the anatomical landmarks in the Grave 6 collection. In contrast, the EBA II-III assemblage from Bab edh ’Dhra was burned, damaged by a roof collapse, commingled, and was subject to poor preservation efforts (Sheridan 2014). While I cannot directly verify the relative condition of the two collections without firsthand experience of the Bab edh ‘Dhra collection, the available reports suggest that the WF100 material is comparatively better preserved.

In contrast, by directly controlling key aspects of my method design – such as landmark selection, managing the ambiguity in element identification, and the use of both subadult bone clones and real subadult skeletal elements – I was able to improve the consistency of the results and enhance the usability of the Landmark System on commingled and fragmentary remains. However, the use of reference materials did present its own challenges. Differences between the bone clones, the UWaterloo subadult bone collection, and the actual Grave 6 remains may have introduced small inconsistencies in landmark recognition, particularly with highly fragmented elements. Some elements were simply too small or damaged to recognize, even with comparison to subadult bone clones and the UWaterloo subadult bone collection. Often times when this became an issue, help from graduate peers, the lab Manager Jeff Coffin, or my advisor Dr. Alexis Dolphin was provided. If assistance was not available or others could not identify what a bone fragment was, subtle modifications to my cataloguing were made to include this. A simple statement on the bone was made in a spreadsheet was made to include the bone that could not be used, what bone it most resembled, and what part of the bone it most resembled.

The Landmark System and its modifications made an MNI estimation possible from and commingled and fragmentary assemblage; however, as with other studies, the results provide a conservative approximation and cannot be interpreted as exact.

6.2 *Age-At-Death (AAD)*

The age-at-death estimations were straightforward to perform and provided a great deal of information on the collection as a whole. By applying methods compiled by Schaefer and colleagues, an interpretive number of individuals were able to be separated into reasonable age ranges. This process enabled the MNI estimate to be refined based on age groups and associated skeletal elements. The AAD estimates added 5 possible individuals to the MNI estimate,

changing it from 17 to 22. I believe the revised number of 22 individuals would be a suitable estimate of the represented individuals buried in Grave 6. When used in tandem with the modified Landmark System, age-at-death can provide a more accurate estimation of the number of individuals present, and will improve once more information can be gained on subadult populations.

6.2.1 *Limitations for Estimating Age-At-Death*

Variability in the age-of-death of individuals interred in Grave 6 at WF100 did make things difficult as bones varied in size, causing some confusion when initial sorting began. It took a keen eye to observe that some elements were prenatal human remains rather than faunal remains. Unfortunately, it is hard to determine exact age-at-death estimations due to the fragmentary nature of this collection. It was particularly difficult to provide accurate age-at-death estimations for more fragile elements of a bone, such as the auxiliary border of the scapula or the flatter area of a *pars lateralis*. These areas were often broken or completely missing and could not be included in giving an accurate estimation. Pictures of broken elements can be found in Appendix B (Figures 66-69).

Another limitation in the AAD methodologies used is the populations the standards are derived from. Grave 6 is studying the EBA IB population in southern Jordan, from roughly 5000 years ago, while the standard published methods used to estimate the age-at-death are using populations from Portugal in the 20th century, male Bosnian war dead from 1995, English documented remains from the 19th century, The Scheuer collection from the University of Dundee, 18th and 19th century remains from Spitalfields, London, multiracial Americans from 1977 to 1979, and 20th century Hungarian fetal remains (Coqueugniot and Weaver 2007; Schaefer 2008; Black and Scheuer 1996; Rissech and Black 2007; Molleson and Cox 1993;

Webb and Suchey 1985; Cardoso 2008; Fazekas and Kosa 1978). Human morphology will vary depending on a number of factors like health, diet, muscle robusticity, cultural practices, and climate (Relethford 1983). There will be a margin of error when comparing those who lived 200 years ago in England to those who lived 5000 years ago in what would be Jordan today. Differences in growth and development from environmental factors, diet, disease, and other stressors can impact the size or skeletal development of similar age, leading to an over- or underestimation of the age-at-death of skeletal elements. These considerations stress that age-at-death estimations must be interpreted conservatively, and the grouping of elements for MNI estimations based on size or developmental stage may cause uncertainty. Another limitation is the lack of data surrounding subadult bone development in certain areas of the body. This is particularly true for the phalanges and *pars basilaris*, as these bones have limited available data for subadults age estimation. This makes it extremely difficult to provide accurate information above a certain age (Fazekas and Kosa 1978). Other bones such as the patella primarily adopt their adult morphology before adolescence, complicating the interpretation of the data found. Despite the limitations addressed, age-at-death provided valuable insight into how old those who were buried at Wadi Faynan 100 were, and improved the accuracy of the MNI estimate for Grave 6.

Chapter 7: Conclusion

This thesis addressed a methodological gap in estimating the Minimum number of Individuals (MNI) in commingled and fragmentary subadult assemblages through the application of a modified Landmark System to include subadult osteology. This allowed for the assessment of fragmentary and commingled elements that produced a more nuanced estimate than traditional MNI approaches. Despite the limitations presented by preservation, commingling, and the challenges of identifying subadult skeletal material, a minimum of 22 individuals were identified.

The results of this study demonstrate that this method is both applicable and valuable for subadult contexts and can be used to revisit previous collections where traditional MNI methods fall short. In doing so, this research contributes to the library osteological methodology by demonstrating how the Landmark System can be adapted to handle fragmentary and commingled subadult assemblages. Additionally, this study provides new data on Grave 6 at WF100, an Early Bronze Age IB archaeological site, offering insight into age-at-death and the organization of burials during the Early Bronze Age in southern Jordan.

This research also explores the importance of ethical engagement with human remains. Working within both Canadian and Jordanian ethical guidelines, the study acknowledges the individual and cultural significance of those represented by the remains and ensures their respectful treatment throughout the research process. By approaching the material with sensitivity to the structural integrity of these remains, and the integrity of the individual themself, this project upholds contemporary standards for ethical research in osteology.

Finally, this study demonstrates the potential for commingled remains—often overlooked in Near Eastern archaeology—to provide meaningful contributions to our understanding of past

populations. By improving methodological approaches and drawing attention to the research potential of fragmentary assemblages, this research not only enhances osteological practice but also encourages broader discussions about the value of human remains in archaeological research.

References

"AAA Statement on Ethics." The American Anthropological Association, 2012. https://americananthro.org/about/policies/statement-on-ethics/.

Adams, Bradley J., and Lyle W. Konigsberg. "Estimation of the Most Likely Number of Individuals from Commingled Human Skeletal Remains." *American Journal of Physical Anthropology* 125, no. 2 (2004): 138–51.

Adams, Russell B., Alexis Dolphin, John Grattan, et al. "Barqa Landscape Project 2023: Preliminary Report to the Department of Antiquities" (2023): 1–28.

Adams, Russell B. "From Farms to Factories: The Development of Copper Production at Faynan, Southern Jordan, During the Early Bronze Age." *Metals and Society* (2002): 21–32.

Adams, Russell B. "Jordan: an archaeological reader." (2008).

Adams, Russell B., Alexis Dolphin, John Grattan, et al. "Barqa Landscape Project 2019: Preliminary Report to the Department of Antiquities" (2019): 1–20.

Adams, Russell B, Hannah A Friedman, James D Anderson, Michael M Homan, J P Grattan, and Lynne M Rouse. "The Barqa Landscape Project, 2009." Essay. In *Walking Through Jordan*, 247–64. Equinox, 2017.

Albert, A.M. and W.R Maples. "Stages of epiphyseal union for thoracic and lumbar vertebral centra as a method of age determination for teenage and young adult skeletons." *Journal of Forensic Sciences* 40,4 (1995): 623–633.

Al-Shorman, Abdullah, and Ali Khwaileh**.** "Burial Practices in Jordan from the Natufians to the Persians." *Estonian Journal of Archaeology* 15 (2) (2011): 88-108.

Bagnall, K.M., P.F. Harris, and P.R.M Jones. "A radiographic study of the human fetal spine. 2. The sequence of development of ossification centers in the vertebral column." *Journal of Anatomy* 124, 3 (1977): 791–802.

Barker, Graeme, Russell Adams, Oliver Creighton, Hwedi el-Rishi, David Gilbertson, John Grattan, Chris Hunt, Paul Newson, Brian Pyatt, and Tim Reynolds. "Chalcolithic and Bronze Age Settlement in Wadi Faynan: Metallurgy and Social Complexity." In *Archaeology and Desertification, The Wadi Faynan Landscape Survey*, 227–69, 2007.

Baker, Brenda J., Tosha L. Dupras, and Matthew W. Tocheri. *The Osteology of Infants and Children.* Texas A & M University Press, 2005.

Birkner, R. (1978). "Normal Radiographic Patterns and Variances of the Human Skeleton– An X-ray Atlas of Adults and Children." Urban and Schwarzenberg, 1978.

Black, Sue, and Louise Scheuer. "Age Estimation from the Clavicle: Methodology Revisited." *American Journal of Physical Anthropology* 100(2) (1996): 331–34.

Bourgeois, Rebecca, L., Valdimir I. Bazaliiskii, Hugh McKenzie, Terence N. Clark, and Angela R. Liverse. “A four-stage approach to re-associating fragmented and commingled human remains.” *Journal of Archaeological Sciences* 37 (2021): 1-12.

Cardoso, H. “Epiphyseal union at the innominate and lower limb in a modern Portuguese skeletal sample, and age estimation in adolescent and young adult male and female skeletons.” *American Journal of Physical Anthropology* 132, 2 (2008): 161-170.

Carstens, M H. “Development of the Craniofacial Blood Supply: Intracranial System.” Essay In *The Embryological Basis of Craniofacial Structure*, 311–414. Springer, 2023.

Chesson, Meredith. “Embodied Memories of Place and People: Death and Society in an Early Urban Community.” *Archeological Papers of the American Anthropological Association* (2001): 100-113.

Chesson, Meredith. "Libraries of the Dead: Early Bronze Age Charnel Houses and Social 1 Identity at Urban Bab edh-Dhra, Jordan." *Journal of Anthropological Archaeology* 18(2) (1999): 137–64.

Chesson, Meredith. “Remembering and Forgetting in Early Bronze Age Mortuary Practices on the Southeastern Dead Sea Plain, Jordan.” In Performing Death *Social Memory, Identity, and Death*, edited by Nicola Laneri. 2007.

Chesson, Meredith, Nathan Goodale. “Population Aggregation, Residential Storage and Socioeconomic Inequality at Early Bronze Age Numayra, Jordan.” *Journal of Anthropological Archaeology* 35 (2014): 117-134.

“CMA Ethical Guidelines 1999.” Canadian Museums Association, 1999. https://www.museums.ca/uploaded/web/docs/ethicsguidelines.pdf.

“Code of Ethics.” The Canadian Association for Physical Anthropology. 2019. https://caba-acab.net/sites/default/files/basic-page/capa-acap_code_of_ethics_-_jan_2019.pdf

Coqueugniot, Hélène, and Timothy D. Weaver. "Brief Communication: Infracranial Maturation in the skeletal collection from Coimbra, Portugal: new aging standards for epiphyseal union Identified Skeletal Collection." *American Journal of Physical Anthropology* 134(3) (2007): 424–29.

Cunningham, Craig, Lousie Schaefer, and Sue Black. *Developmental Juvenile Osteology: Second Edition.* Academic Press, 2016.

Department of Antiquities of Jordan. Law of Antiquities-Jordan, 2004. https://publication.doa.gov.jo/Publications/ViewPublic/203

DiBiase, Serena. “An Osteological Study of the Individuals Buried in Grave 3 at Wadi Faynan 100, Jordan.” Master’s Thesis, University of Waterloo, 2021.

Fernández-Tresguerres Velasco, J. A. “Jabal al- Mutawwaq at the end of the fourth millennium BC, Studies in the History and Archeology of Jordan.” *SHAJ*, VII (2001): 173-178.

Fernández-Tresguerres Velasco, J. A., The “Temple of the Serpents”, a Sanctuary of the Early Bronze F I in the village of Jabal al-Muṭawwaq (Jordan), *Annual of the Department of Antiquities of Jordan* 52, (2008): 23-34.

Fazekas, István G., and Ferenc Kósa. *Forensic Fetal Osteology.* Budapest: Akadémiai Kiadó. 1978.

Garn, S.M., C. G Rohmann, and F.N. Silverman. “Radiographic standards for postnatal ossification and tooth calcification.” Medical Radiography and Photography 43(1967):45–66.

Gregoricka, Lesley A., Jaime Ullinger, and Susan G. Sheridan. “Status, Kinship, and Place of Burial at Early Bronze Age Bab Adh-dhra’: A Biogeochemical Comparison of Charnel House Human Remains.” *American Journal of Physical Anthropology* 171, no. 2 (2019): 319–35.

“Human Remains.” Parks Canada Agency, Government of Canada., November 26, 2022. https://parks.canada.ca/docs/r/pfa-fap/sec7/decouv_discov3.

Kafafi, Zeidan A. “Archaeological Sites and Local Communities in Jordan: An Example from Tell Deir ’Alla.” *Egyptian Journal of Archaeological and Restoration Studies* 11, no. 1 (2021): 1–7.

Knüsel, Christopher J., and Alan K. Outram. “Fragmentation: The Zonation Method Applied to Fragmented Human Remains from Archaeological and Forensic Contexts.” *Environmental Archaeology* 9, no. 1 (2004): 85–98.

Kreissl Lonfat, Bettina, Ina Maria Kaufmann, Frank Rühli. “A Code of Ethics for Evidence Based Research with Ancient Humans Remains.” *The Anatomical Record* 298, 6 (2015): 1175-1181.

Lambacher, Nicole, Karina Gerdau-Radonic, Emma Bonthorne, and Francisco José Valle de Tarazaga Montero. “Evaluating Three Methods to Estimate the Number of Individuals from a Commingled Context.” *Journal of Archaeological Science: Reports* 10 (2016): 674–83. https://doi.org/10.1016/j.jasrep.2016.07.008.

Lewis, Mary E. "The Bioarchaeology of Children." in *The Bioarchaeology of Children: Perspectives from Biological and Forensic Anthropology*. Cambridge University Press, 2007.

Licata, Marta, Alessandro Bonsignore, Rosa Boano, and Francesca Monza. “Study, Conservation and Exhibition of Human Remains: The Need of a Bioethical Perspective.” *Medical Humanities* 91, no. 4 (2020): 1–10.

Mack, J. E., A. J. Waterman, A-M. Racila, J. A. Artz, and K. T. Lillios. “Applying Zooarchaeological Methods to Interpret Mortuary Behaviour and Taphonomy in

Commingled Burials: The Case Study of the Late Neolithic Site of Bolores, Portugal." *International Journal of Osteoarchaeology* 26, no. 3 (2015): 524–36.

Mitchell, Piers D., and Megan Brickley, eds. "Guidelines to the Standards for Recording Human Remains." British Association for Biological Anthropology and Osteoarchaeology, 2017.

Molleson, Theya, and Margaret Cox. *The Spitalfields Project Volume 2: The Anthropology – The Middling Sort.* York: Council for British Archaeology. 1993

Moorrees, C., E. Fanning and E Hunt. "Age variation of formation stages for ten permanent teeth." *Dental Research* 42, 6 (1963): 1460-1502.

Morton, Robert J, and D Wayne. "Detection and Recovery of Abducted and Murdered Children: Behavioral and Taphonomic Influences." Essay. In *Advances in Forensic Taphonomy*, 151–71. CRC Press, 2001.

Muniz, Juan, Andrea Polcaro, Valentin Alvarez. "New Spanish - Italian Excavations at the Jebel al-Mutawwaq Dolmen Field on the Middle Wadi az-Zarqa: Preliminary Results of the 2012 Season". *Studies in the History and Archaeology of Jordan XII, Amman,* (2016): 477-488**.**

National Cancer Institute. 2025. "Anatomy of the Human Skeleton." Accessed March 25, 2025.

Ortner, D. J., and B. Frohlich. "The Eb IA Tombs and Burials of Bâb Edh-Dhrâ, Jordan: A Bioarchaeological Perspective on the People." *International Journal of Osteoarchaeology* 17, no. 4 (2007): 358–68.

Palmiotto, Andrea, Heli Maijanen, Carrie B. LeGarde, and Megan Ingvolstad. "Advances in commingled human remains analysis between 2014 and 2023". *Journal of Forensic Science* 69(5) (2024): 1604-1619.

Philip, Graham. "The Early Brone Age I-III" in *The Archaeology of Jordan,* edited by Burton MacDonald, Russell Adams, and Piotr Bienkowski. Sheffield Academic Press, 2001.

Polcaro, Andrea, Juan Muniz. "Preliminary Report on the Seventh Season (2018) of Spanish-Italian Excavations at Jabal Al-Mutawwaq, Wadi Az-Zarqa', Jordan", *Annual of the Department of Antiquities of Jordan* 60, (2022):301-310.

Polcaro, Andrea, Juan Muñiz, Valentín Alvarez, and Silvia Mogliazza. "Dolmen 317 and Its Hidden Burial: An Early Bronze Age I Megalithic Tomb from Jebel al-Mutawwaq (Jordan)." *Bulletin of the American Schools of Oriental Research* 372 (2014): 1–17.

"Prevention of Illicit Trafficking of Cultural Property - Learning Materials." Acor Jordan, September 27, 2023. https://acorjordan.org/prevention-of-illicit-trafficking-resources/.

"Principles of Ethical Conduct." Canadian Archaeological Association, 2022.

Pyatt, F.B., A.J. Pyatt, C. Walker, T. Sheen, and J.P. Grattan. "The Heavy Metal Content of Skeletons from an Ancient Metalliferous Polluted Area in Southern Jordan with Particular

Reference to Bioaccumulation and Human Health." *Ecotoxicology and Environmental Safety* 60, no. 3 (2005): 295–300.

Radziwiłko, Katarzyna, Łukasz Kutyło, and Piotr Kołodziejczyk. "Archaeological Research as a Benefit for the Local Community: Southern Jordan as a Preliminary Socioarchaeology Study." *Studies in Ancient Art and Civilisation* 24 (2020): 205–25.

Rast, Walter E., and R. Thomas Schaub. *Bab edh-Dhra: Excavations in the Cemetery Directed by Paul W. Lapp (1965–67).* Winona Lake, IN: Eisenbrauns. 1981.

Relethford, John H. "Population Structure and the Genetic Analysis of Skeletal Samples." *American Journal of Physical Anthropology* 62(4) (1983): 473–82.

Rissech, C. and Black, S. "Scapular development from the neonatal period to skeletal maturity: A preliminary study." International Journal of Osteoarchaeology 17(5):451–464.

Ronza, Maria. "Do Communities Have a Role in Community Archaeology in Jordan?" in *Living Communities and Their Archaeologies in the Middle East*. 2023.

Ruddell, Kasi. "Echoes of Contamination: Investigating heavy metal exposure at Wadi Faynan 100, Jordan." Master's Thesis, University of Waterloo, 2025.

Schaefer, Maureen. "A summary of epiphyseal union timing in Bosnian males." *International Journal of Osteoarchaeology.* 2008.

Schaefer, Maureen, Sue M. Black, and Louise Scheuer. *Juvenile osteology: A laboratory and field manual*. Amsterdam: Academic, 2009.

Scheuer, Louise, and Sue MacLaughlin-Black. "Age Estimation from the Pars Basilaris of the Fetal and Juvenile Occipital Bone." *International Journal of Osteoarchaeology* 4, no. 4 (1994): 377–80.

Sheridan, Susan Guise. "Bioarchaeology in the Ancient Near East: Challenges and Future Directions for the Southern Levant." *American Journal of Physical Anthropology* 162, no. S63 (2017): 110–52.

Sheridan, Susan Guise, Jaime Ullinger, Lesley Gregoricka, and Meredith S. Chesson. "Bioarchaeological Reconstruction of Group Identity at Early Bronze Age Bab Edh-Dhra', Jordan." In *Remembering the Dead in the Ancient Near East: Recent Contributions from Bioarchaeology and Mortuary Archaeology*, edited by Benjamin W. Porter and Alexis T. Boutin. University Press of Colorado, 2014.

"Statement Concerning the Treatment of Human Remains." Society for American Anthropology, 2021.

Squires, Kirsty., David Errickson, Nicholas Marquez-Grant. *Ethical Approaches to Human Remains A Global Challenge in Bioarchaeology and Forensic Anthropology: A Global Challenge in Bioarchaeology and Forensic Anthropology*. 2019.

Tan, Kaithleen. “A Trace Element Analysis of Lead in Human Tooth Enamel from Wadi Faynan 100, Jordan.” Master’s Thesis, University of Waterloo, 2022.

Tirpan, Sevil., “Minding the Gap: Attempts at Community Archaeology and Local Counter-Narratives at an Archaeological Site in Turkey.” *Journal of Social Archaeology* 22 (3) (2022): 235-254.

“Tri-Council Policy Statement: Ethical Conduct for Research Involving Humans.” Canadian Institutes of Health Research, Natural Sciences and Engineering Research Council of Canada, and Social Sciences and Humanities Research Council, 2022.

Tucciarone, Julia. “A Comprehensive analysis of Dental Remains from the Early Bronze Age I site of Wadi Faynan 100, Jordan.” Master’s Thesis, University of Waterloo, 2020.

Ullinger, Jaime M., Susan G. Sheridan, and Donald J. Ortner. “Daily Activity and Lower Limb Modification at Bab Edh-Dhrȧ, Jordan, in the Early Bronze Age.” *Bioarchaeology and Behavior*. (2013): 180–202.

Vaduveskovic, Igor, and Marija Djuric. "Mass grave complexity effects on the minimum number of individuals estimation." *Forensic Science, Medicine and Pathology* 16(1) (2020): 57–64.

Van den Dries, M.H. *“*The Public Benefits of Archaeology According to the Public.” *Internet Archaeology* 57 (2021).

Vieira, Olivia. “Skeletal Trauma Analysis of an Early Bronze Age Population at Wadi Faynan 100, Jordan.” Master’s Thesis, University of Waterloo, 2025.

Webb, Patricia A.O., and John M. Suchey. "Epiphyseal Union of the Anterior Iliac Crest and medial clavicle in a modern multiracial sample of American males and females." *American Journal of Physical Anthropology* 68(4) (1985): 457–66.

White, Theodore E. “A Method of Calculating the Dietary Percentage of Various Food Animals Utilized by Aboriginal Peoples.” *American Antiquity* 18, no. 4 (1953): 396–98. https://doi.org/10.2307/277116.

White, Tim., Pieter A. Folkens. *The Human Bone Manual*. Elsevier Academic Press, 2005.

Wright, Katherine, Mohammed Najjar, Jonathan Last, et al. “The Wadi Faynan Fourth and Third Millennia Project, 1997: Report on the First Season of Test Excavations at Wadi Faynan 100.”, *Levant* 30 no. 1:(1998) 33-60.

Appendix A – *Landmark System Reference Guide*

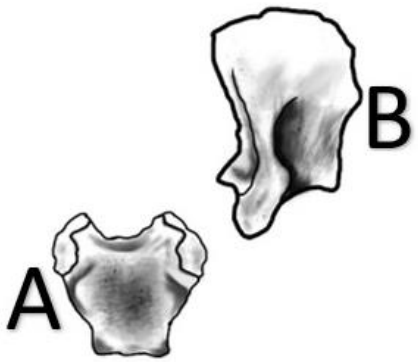


Figure 32. Pars Basilaris (A) and Pars Lateralis (B) Elements are shown before fusing with the occipital bone. Internal View.



Figure 33. Left Temporal (A). Internal View.



Figure 34. Vertebrae, General Neural Arch (A). Inferior View. Image based on Cervical Vertebra neural arch.



Figure 35. Vertebrae, General Centrum (Body) (A) Superior View. Image based on Lumbar Vertebra centrum.

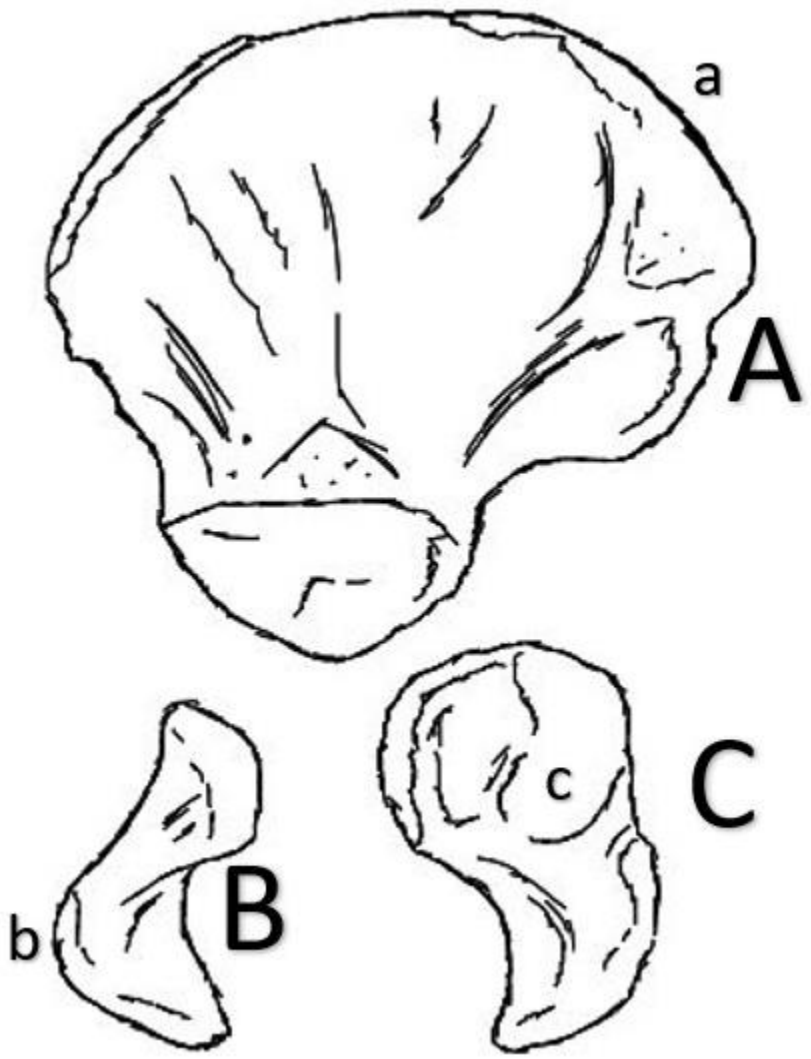


Figure 36. Left Os coxa. A (ilium), B (pubis), C (ischium), a (iliac crest), b (pubic symphysis), c (lunate surface). Lateral View.

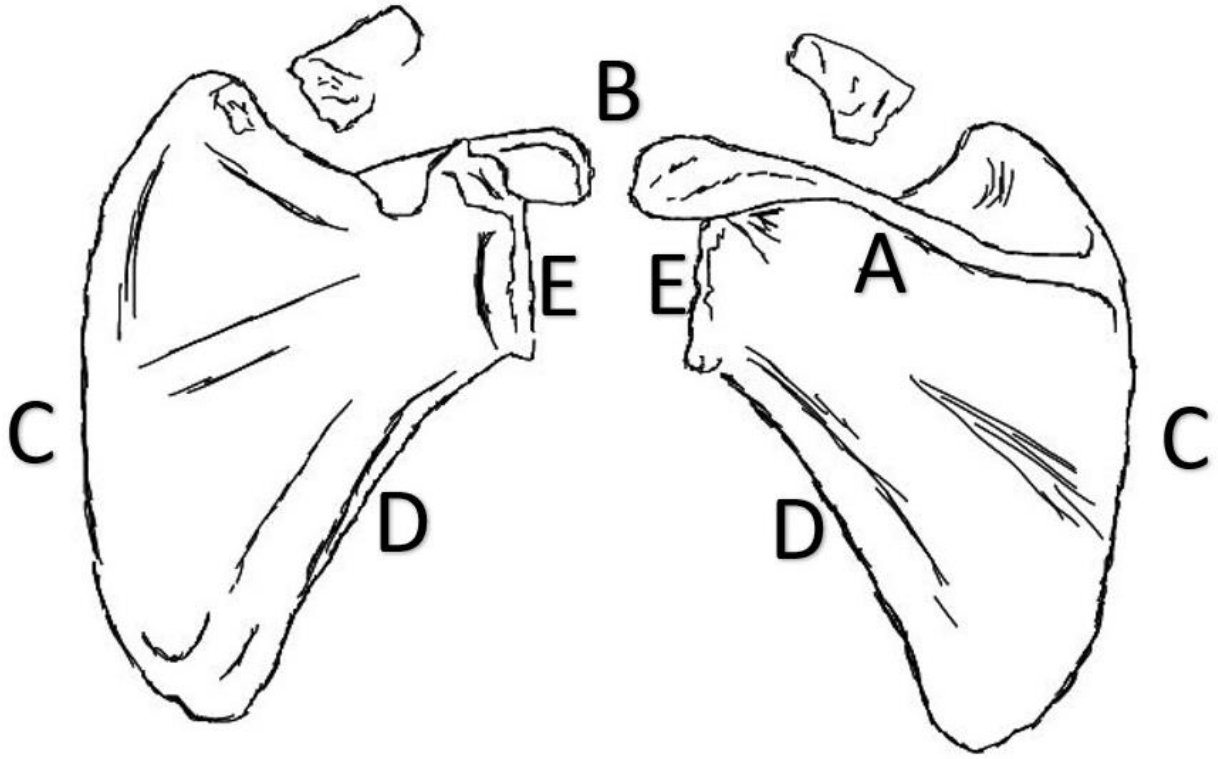


Figure 37. Left Scapula. A (scapular spine), B (acromion process), C (medial boarder), D (lateral boarder), E (glenoid cavity). Left = Anterior, Right = Posterior View.

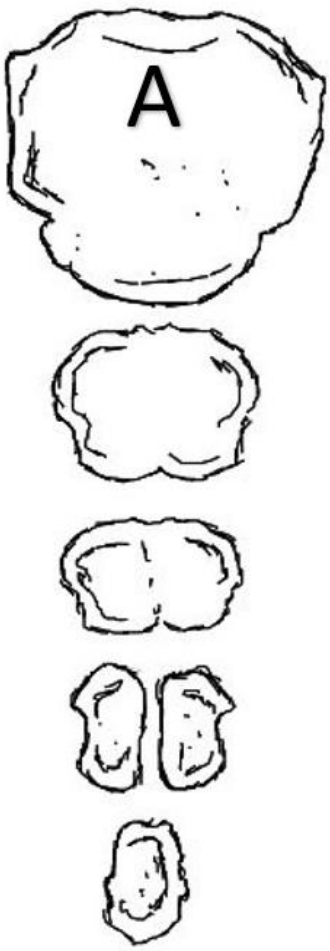


Figure 38. Sternum. A (Manubrium). Anterior View.

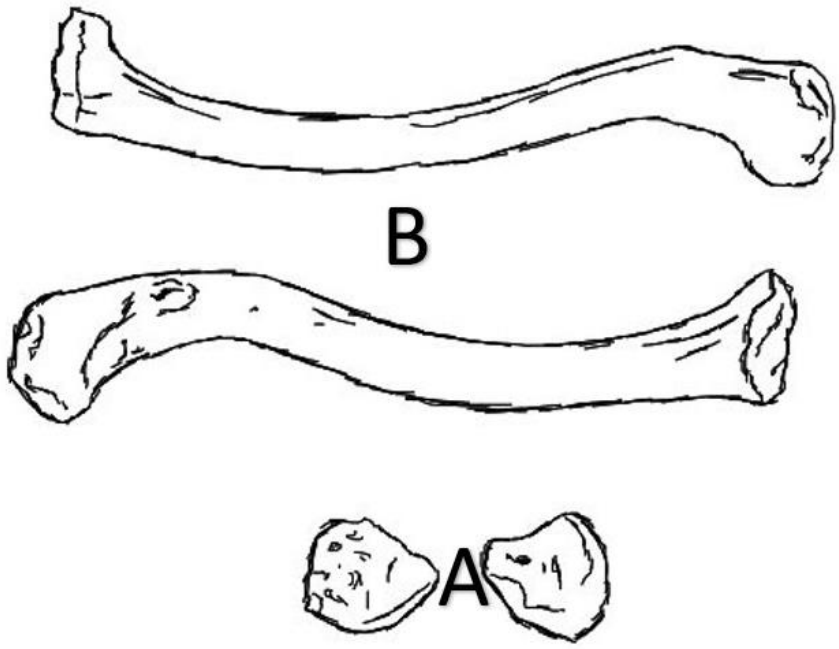


Figure 39. Left Clavicle. A (Medial epiphysis), B (shaft). Top = Superior View, Bottom = Metaphyseal View (left) and Medial View (right).

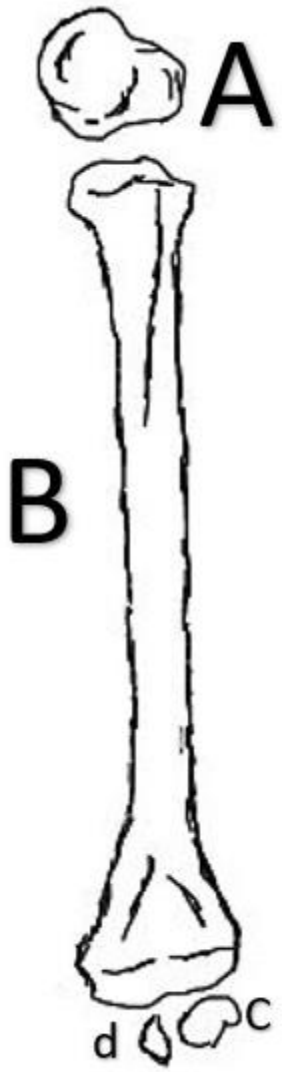


Figure 40. Left Humerus. A (Proximal epiphysis/head), B (shaft), c (capitulum), d (trochlea). Anterior View.

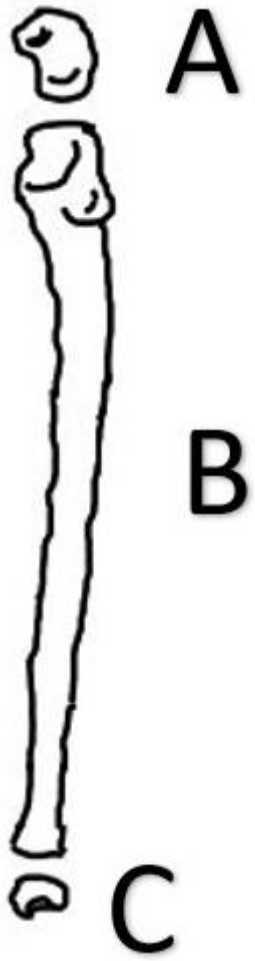


Figure 41. Left Ulna. A (proximal epiphysis), B (Shaft), C (distal epiphysis). Anterior View.



Figure 42. Left Radius. A (proximal epiphysis), B (Shaft), C (distal epiphysis). Anterior View.

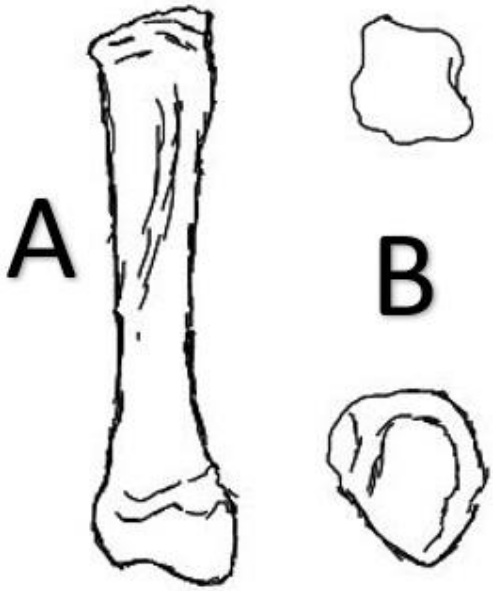


Figure 43. Right Second Metacarpal. A (Metacarpal), B (Metacarpal epiphysis). Dorsal View of Shaft. Top Epiphysis = Distal View, Bottom Epiphysis= Proximal Views.

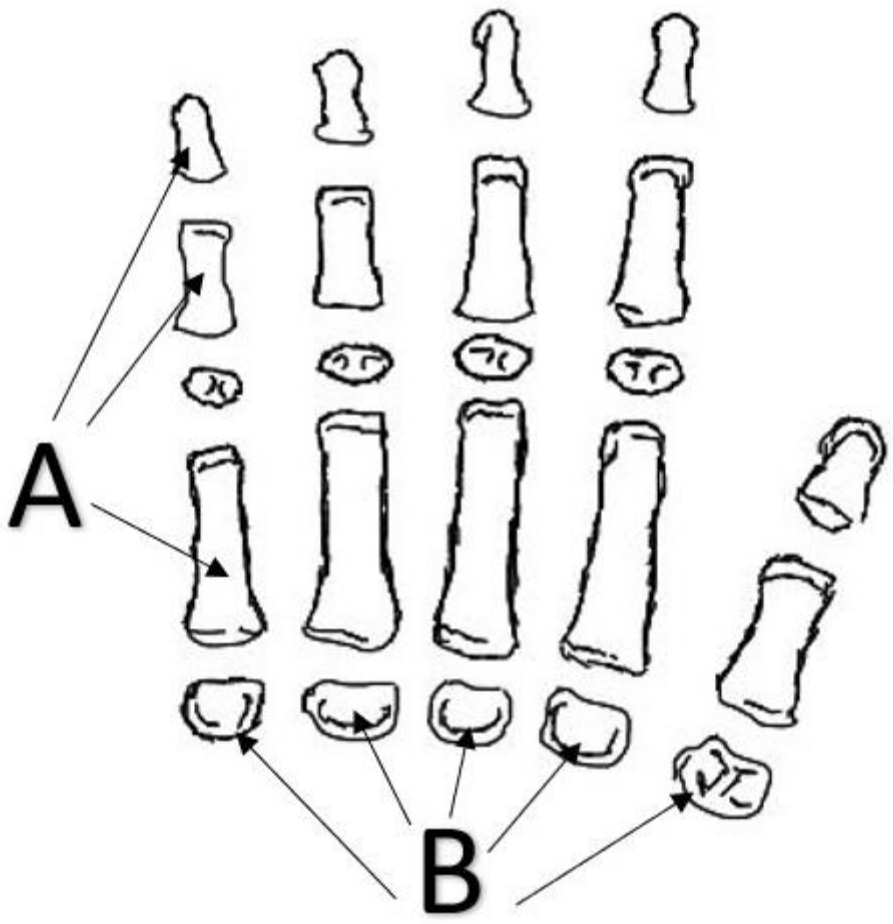


Figure 44. Left Hand of subadult. A (phalanx) B (Phalanx epiphysis). Shafts = Dorsal View; Epiphyses = Proximal View.



Figure 45. Left Scaphoid.



Figure 46. Left Lunate.

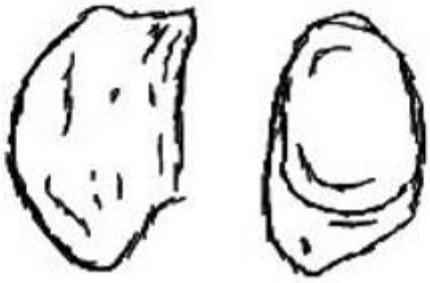


Figure 47. Left Pisiform.



Figure 48. Left Triquetral.

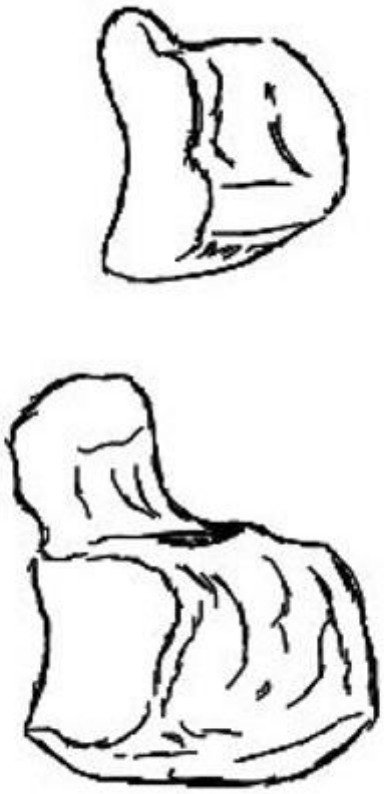


Figure 49. Left Hamate.



Figure 50. Left Trapezium.

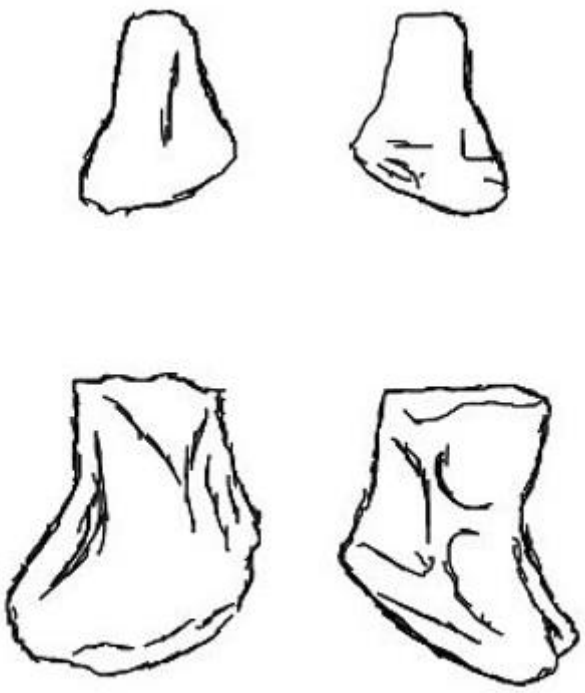


Figure 51. Left Trapezoid.

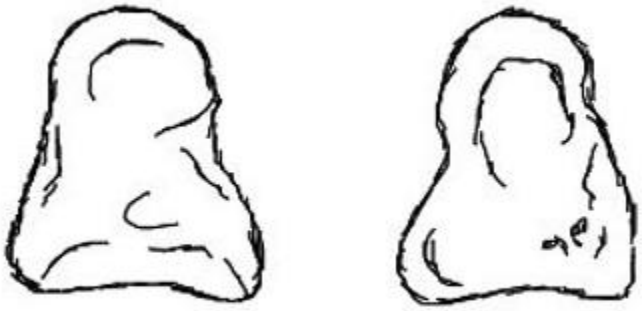


Figure 52. Left Capitate.

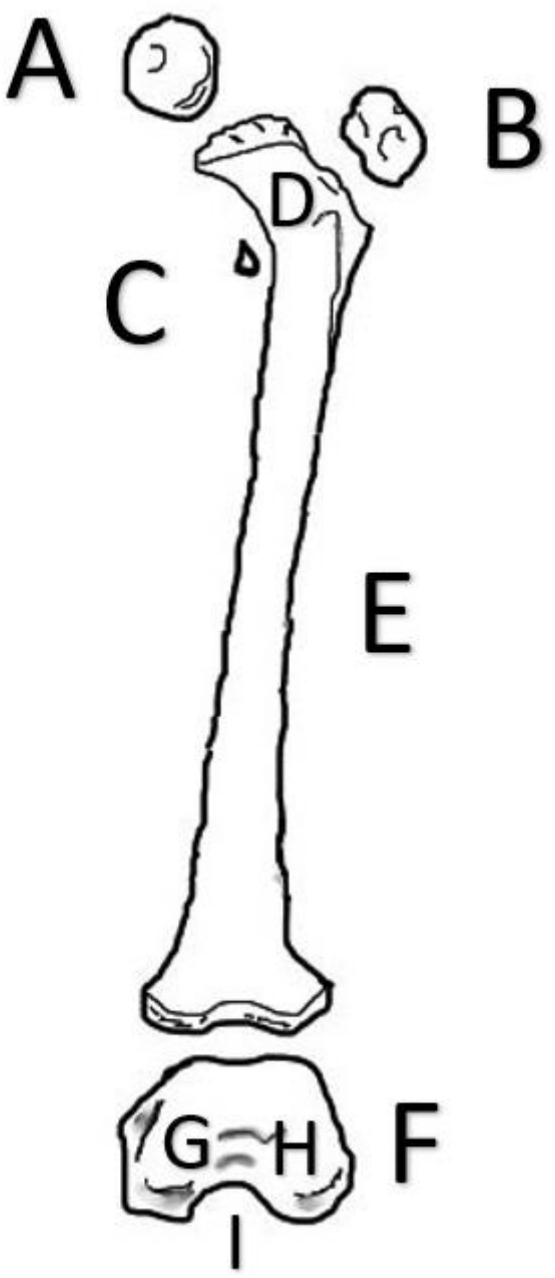


Figure 53. Left Femur. A (Head/proximal epiphysis), B (greater trochanter), C (lesser trochanter), D (neck), E (Shaft), F (Distal epiphysis), G (medial condyle, H (lateral condyle), I (intercondylar fossa). Anterior View.

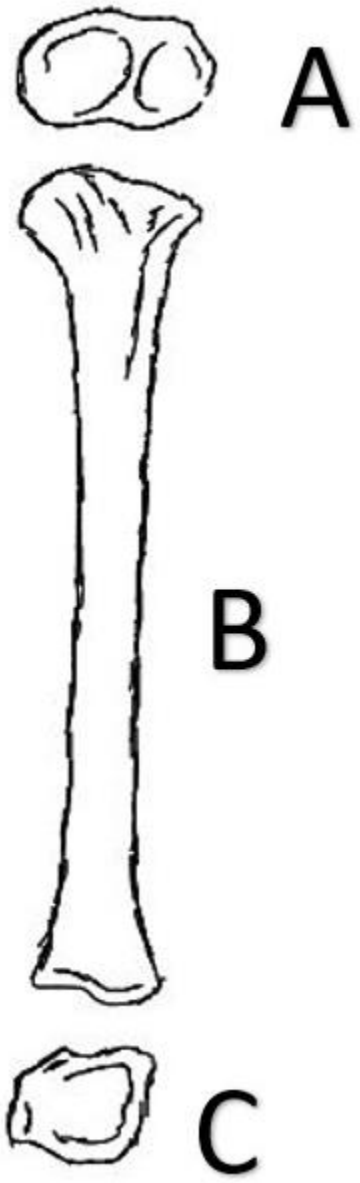


Figure 54. Left Tibia. A (proximal epiphysis), B (shaft), C (distal epiphysis). Anterior View.

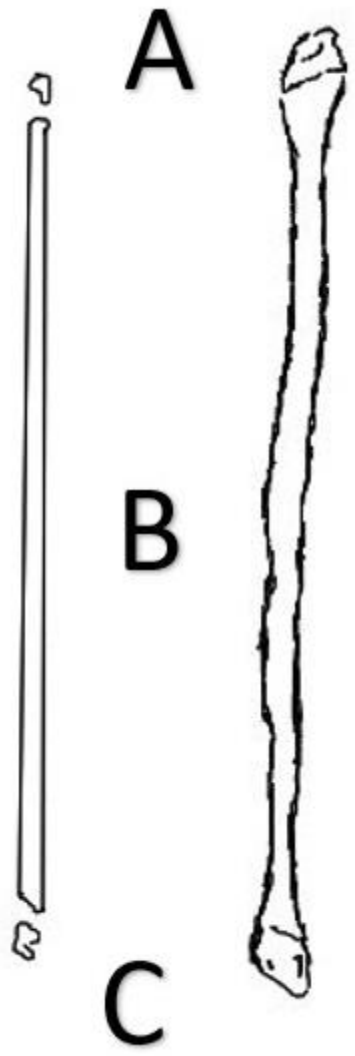


Figure 55. Left Fibula. A (proximal epiphysis), B (shaft), C (distal epiphysis). Anterior View.

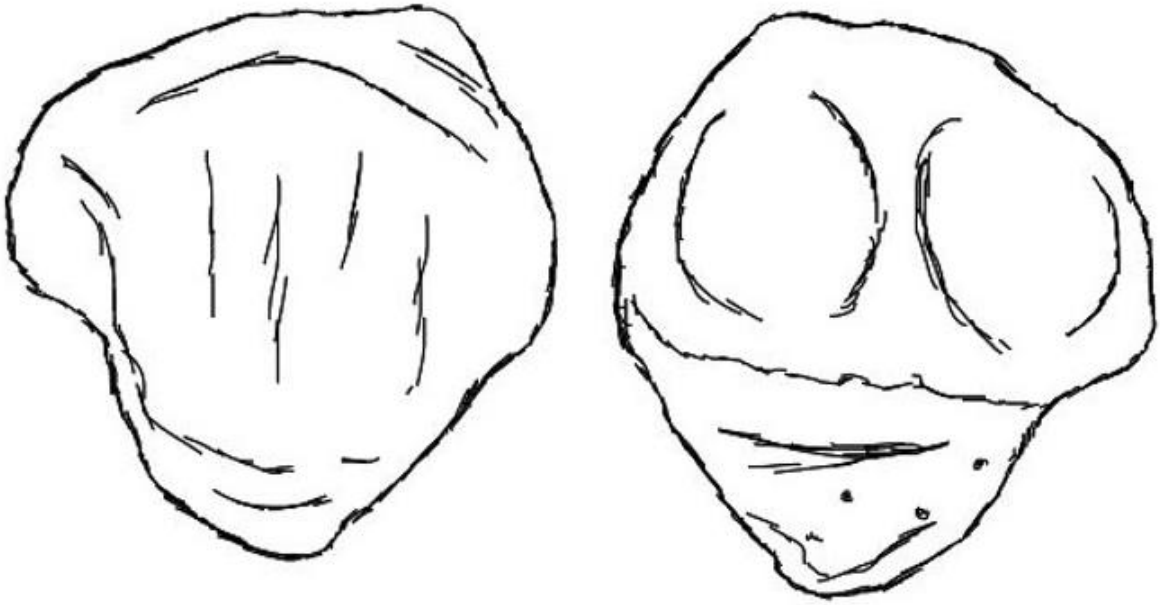


Figure 56. Left Patella. Left = Anterior View, Right = Posterior View.

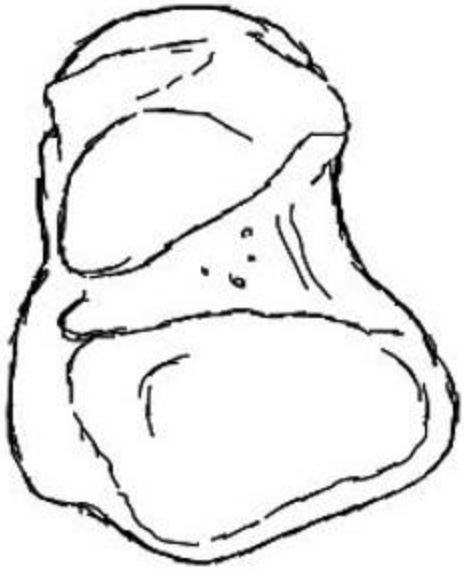


Figure 57. Left Talus. Inferior View.



Figure 58. Left Calcaneus. A (calcaneus epiphysis). Superior View.



Figure 59. Left Cuboid. Dorsal View.

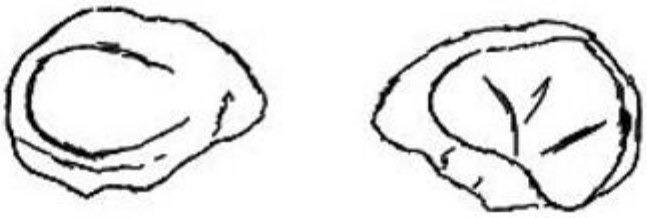


Figure 60. Left Navicular. Left = Proximal View, Right = Distal View.



Figure 61. Left First Cuneiform. Lateral View.



Figure 62. Left Second Cuneiform. Lateral View.



Figure 63. Left Third Cuneiform. Medial View.

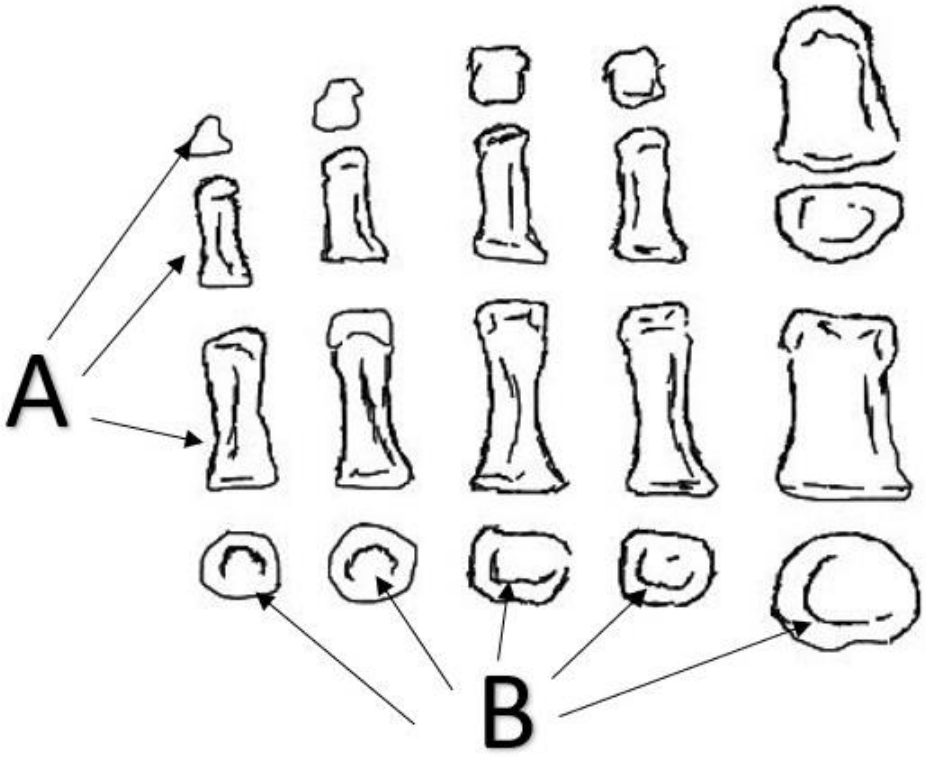


Figure 64. Left Subadult foot. A (Phalanx), B (Phalanx epiphysis). Shafts = Dorsal View, Epiphyses = Proximal View.

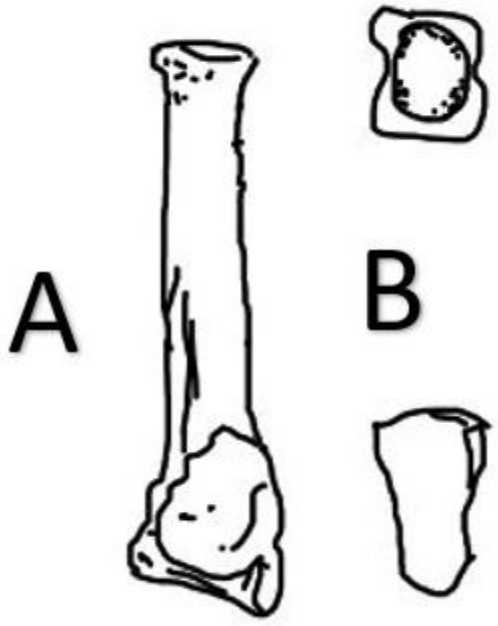


Figure 65. Right Second Metatarsal. A (Metatarsal), B (Metatarsal epiphysis). Shaft = Dorsal View, Epiphysis Top = Distal View, Epiphysis Bottom = Proximal View.

Appendix B – ***Photos of the Wadi Faynan 100 Grave 6 Subadult Collection***

This Appendix showcases 4 examples of the broken bone that was worked on in this thesis. Figure 38 and 39 were able to be identified, while figure 40 and 41 were not. All four examples communicate the extent of damage the subadult remains sustained in Grave 6.

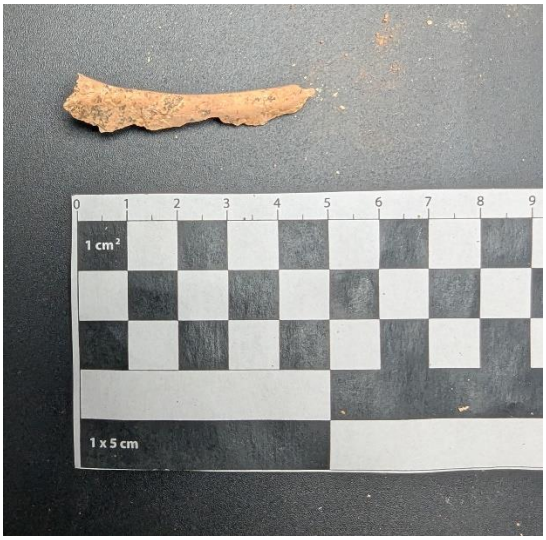


Figure 66. Lateral Border of Subadult Scapula



Figure 67. Subadult Pars Lateralis



Figure 68. Subadult Miscellaneous Squama



Figure 69. Subadult Miscellaneous Long Bone Fragment